frontiers in Materials

REVIEW
published: 30 June 2020
doi: 10.3389/fmats.2020.00147

Advances in Layered Double Hydroxide/Carbon Nanocomposites Containing Ni^{2+} and $Co^{2+/3+}$ for Supercapacitors

Shalini Kulandaivalu[1], *Nur Hawa Nabilah Azman*[1] *and Yusran Sulaiman*[1,2]*

[1] Department of Chemistry, Faculty of Science, Universiti Putra Malaysia, Serdang, Malaysia, [2] Functional Devices Laboratory, Institute of Advanced Technology, Universiti Putra Malaysia, Serdang, Malaysia

The exceptional characteristics and uniqueness of two-dimensional nickel-cobalt layered double hydroxides (Ni-Co LDHs) make them highly desirable material for supercapacitors. A combination of Ni-Co LDHs with carbon-based materials has given stupendous improvement to the performance of supercapacitors in terms of specific energy, specific capacitance, and specific power. Herein, a comprehensive insight into the recent progress of Ni-Co LDHs/carbon composites for supercapacitors is provided to the readers. Beginning with the description on the classification of supercapacitors and the detailed explanation on LDHs and carbon materials. The morphology, properties and electrochemical performances of the Ni-Co LDHs/carbon composites are well-elaborated in this review. The review also discusses the structural identification and important factors that influence the synthesis of LDHs.

Keywords: layered double hydroxides, supercapacitor, carbon materials, nickel, cobalt

OPEN ACCESS

Edited by:
Federico Cesano,
University of Turin, Italy

Reviewed by:
Cheng Jp,
Zhejiang University, China
Zan Gao,
University of Virginia, United States
David Aradilla,
Commissariat à l'Energie Atomique et aux Energies Alternatives (CEA), France

***Correspondence:**
Yusran Sulaiman
yusran@upm.edu.my

Specialty section:
This article was submitted to Energy Materials, a section of the journal Frontiers in Materials

Received: *19 December 2019*
Accepted: *27 April 2020*
Published: *30 June 2020*

Citation:
Kulandaivalu S, Azman NHN and Sulaiman Y (2020) Advances in Layered Double Hydroxide/Carbon Nanocomposites Containing Ni^{2+} and $Co^{2+/3+}$ for Supercapacitors. Front. Mater. 7:147. doi: 10.3389/fmats.2020.00147

INTRODUCTION

Abundant fossil fuels in the earth converted agricultural society to an industrial society, known as the industrial revolution. Since then, due to the growing need for energy to support economic growth and sustainable society, non-renewable fossil fuels are limited in supply. Based on the report provided in the British Petroleum (BP) Statistical Review of World Energy 2018 by the BP Company PLC, the growth of global primary energy consumption was estimated to increase in the rate of 2.2% as of 2017 and, the world set the highest fuel consumption record for natural gas (BP, 2018). Throughout industrialization, an alarming level of fossil fuel consumption is associated with environmental issues. The massive carbon dioxide emission from fossil fuel consumption has caused major climate change faced by today's world and this is also responsible for global warming and pollutions. This has triggered the quest for effective usage of renewable energy sources to replace fossil fuels. Despite the cost and efficiency, energy storage is the main hurdle in keeping up with renewable energies. Therefore, electrochemical energy storage systems are usually integrated with renewable energy sources to store and to deliver the energies efficiently. In that context, the development of nanotechnology, exploration for nano-sized materials, devices and systems has shed light on producing energy conversion and storage systems. Notably, in recent years, many significant efforts have been devoted to developing next-generation high-performance energy storage devices, particularly electrochemical supercapacitors. In 1957, General Electric had introduced the first double layer capacitor and patented the work (Becker, 1957). However, the outbreak of the era of supercapacitors is from Standard Oil of Ohio (SOHIO) when they

commercialized double layer supercapacitors as an official energy storage device (Pandolfo and Hollenkamp, 2006). Since then, it continues to tempt the attention of scientific communities as pointed by the number of articles published in supercapacitors (**Figures 1A,B**). To date, the devices exemplified as state-of-the-art for its impressive performance and also regarded as a highly promising electrochemical energy storage system among the available energy storage devices. It has unearthed profound impacts on today's world.

ELECTROCHEMICAL SUPERCAPACITOR

Electrochemical supercapacitors or more commonly known as supercapacitors differ from conventional capacitors in terms of performance. Generally, conventional capacitors and supercapacitors are governed by the same principals. Both systems are separated by a separator between the two conductive electrodes. However, the separator in the conventional capacitor is an insulating dielectric material, for instance, ceramic and glass. Contrarily, in supercapacitors, the two conductive electrodes are separated by a permeable insulating separator soaked in an electrolyte. Adding to this, the conductive electrodes of a supercapacitor mainly consists of highly porous electrodes with a high surface area instead of planar plates used in conventional capacitors. The permeable separator in supercapacitors allows ions from the electrolyte to move across the separator penetrating the material utilizing the porosity upon electrode polarization (**Figure 1C**). Whereas, when the electrodes are polarized in conventional capacitors, the charges will accumulate along the surface of dielectric material, creating electric fields as shown in **Figure 1D** (Kim et al., 2015). The superiority of supercapacitors accessing the porosity of electrodes makes it better performance than conventional capacitors.

The principles of supercapacitors have been widely reviewed in literature (Wang et al., 2012; Yu et al., 2015; Liu et al., 2018a). Briefly, supercapacitors are classified into two types, electrochemical double layer capacitors (EDLCs) and pseudocapacitors based on their charge storage mechanisms.

i. EDLCs stores energy by forming an electrochemical double layer at the interface of an electrode and electrolyte. An EDLC utilizes high-surface-area carbon-based materials as electrodes. It has excellent cycling stability that is able

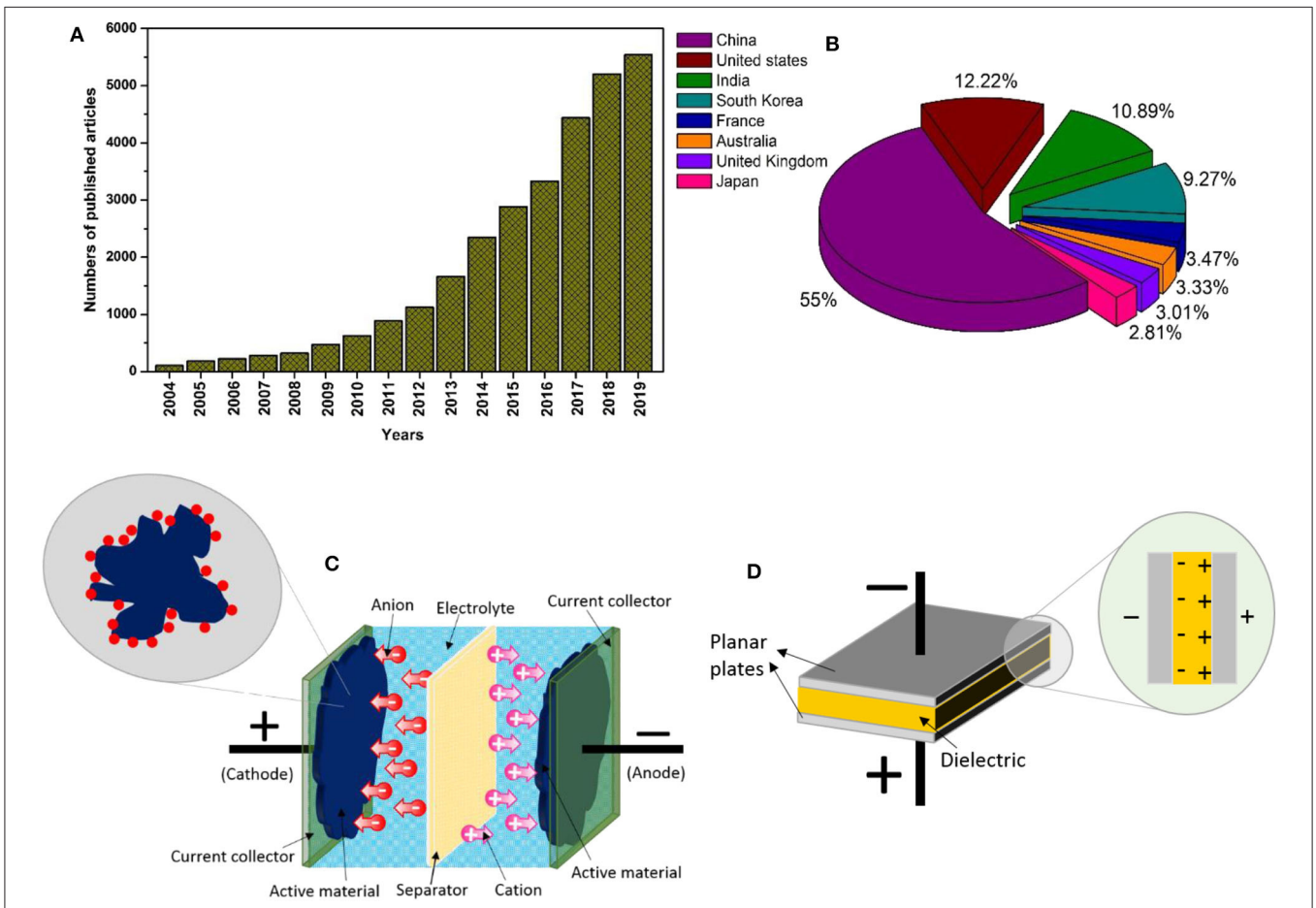

FIGURE 1 | (A) Trends in the number of articles published on supercapacitor, **(B)** proportions of overall publications by countries from 2004 to 2019 using the keyword "supercapacitor." (Data is collected from Scopus on 30 November 2019.), **(C)** schematic diagram of electrochemical supercapacitor, and **(D)** conventional capacitor.

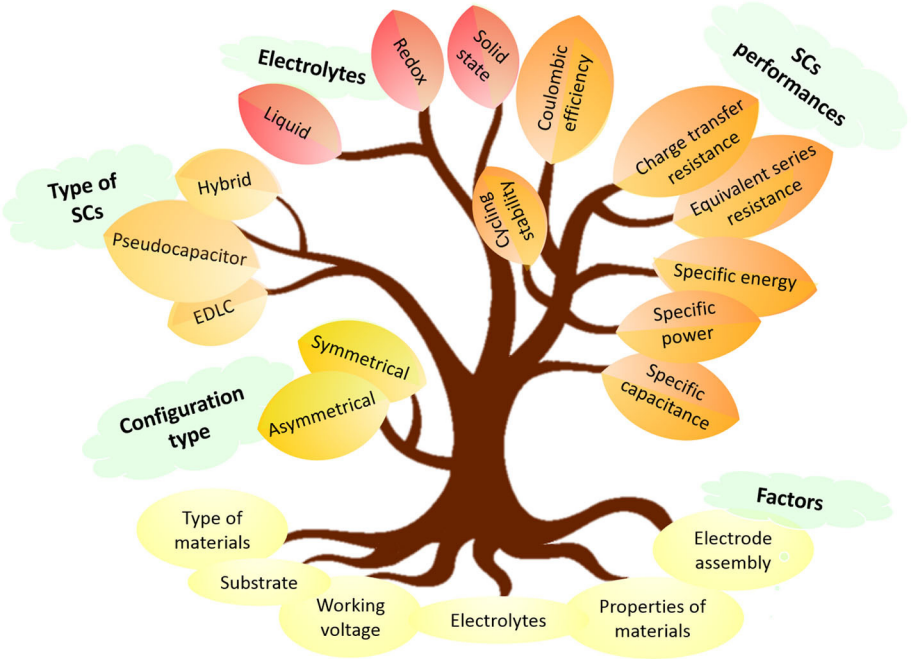

FIGURE 2 | Configuration, types, performance, and factor affecting electrochemical performance of supercapacitors.

to withstand a thousand continuous cycles without any significant changes in performance. However, EDLC has inadequate specific energy (Simon and Gogotsi, 2008).

ii. The charge storage of pseudocapacitors is based on the fast and reversible redox reactions of electroactive materials. Conducting polymers and transition metal oxides/hydroxides are common pseudocapacitive materials. In contrary to EDLC, pseudocapacitors have excellent specific capacitance. However, the poor cycling stability of pseudocapacitors due to the reversible oxidation-reduction reaction at/or near the electrode surface causing swelling and shrinkage of the materials. As a consequence, pseudocapacitors exhibit lower specific power performance than EDLC (Simon and Gogotsi, 2008).

By combining the energy storage mechanisms of EDLCs and pseudocapacitors, hybrid supercapacitors are produced. Hybrid supercapacitors were introduced as an effort to enhance the performance of the existing EDLCs and pseudocapacitors. It can be assembled symmetrically or asymmetrically depending on the configuration assembly (**Figure 2**). A symmetrical supercapacitor is configured with two similar electrode materials consisting of EDLC materials or pseudocapacitive materials (Sun et al., 2017). Whereas, an asymmetrical supercapacitor is made with different anode and cathode electrode materials (Fan et al., 2011). Theoretically, hybrid supercapacitors have better energy storage performances than EDLCs and pseudocapacitors (Kulandaivalu and Sulaiman, 2019). The alluring characteristics of electrochemical supercapacitors outperformed the lithium-ion batteries in terms of its high specific power (> 10 kW kg^{-1}), fast charging-discharging abilities (within few seconds) and long shelf life (>100,000 cycles) (Liu et al., 2016). However, it is still competing with lithium-ion batteries to achieve better specific energy.

Pointing on the specific energy and specific power, these two are the most imperative parameters comparing the performances of energy storage systems and it is commonly represented in a chart known as the Ragone plot. The specific energy (Wh kg^{-1}) typifies the energy capacity that the device is able to hold, whereas specific power (W kg^{-1}) represents the rate of the energy deliverable at a constant current density. This information is usually derived from galvanostatic charge-discharge (GCD) curves by the following equations:

$$Specific\ energy = \frac{0.5 \times (\Delta V^2) \times C_{sp}}{3.6} \quad (1)$$

$$Specific\ power = \frac{E \times 3600}{\Delta t} \quad (2)$$

where ΔV is cell operation potential, C_{sp} is specific capacitance, E is specific energy and Δt is the discharge time (Luan et al., 2013). Based on Equation (1), specific energy can be enhanced by increasing the specific capacitance and cell operation potential (Guo et al., 2019b). The ability of the materials to accommodate the charges is reflected by the specific capacitance. Hence, the electrode material is significantly important to enhance the specific capacitance. Selecting electrode materials should be placed equally on the porosity and surface area of the materials (Shi et al., 2011). However, it is worth to note, not all the surface area of the materials is accessible to the ions from the electrolytes (Lobato et al., 2017). Therefore, the effective surface area is the most accurate term to describe the influence

of the surface area of materials on the specific capacitance enhancement. Notably, pore size playing a crucial role for the electrolyte ion accessibilities within the materials utilizing the surface area, and thus increases the specific capacitance. Young et al. (2018) reported that the pore size of materials should be larger than the size of electrolyte ions for ions penetration. However, the best or suitable material pore size is still in disagreements (Largeot et al., 2008); thus, the authors concluded that each electrode material has its own critical pore size for ion penetration. Additionally, the electrode materials should also possess good electrical conductivity and satisfactory stability for high-performance supercapacitors. Apart from this, an alternative approach to increase the specific capacitance is by widening the cell operation potential. The operating potential of a supercapacitor relies on electrolyte (Pandolfo and Hollenkamp, 2006). The selection of electrolytes is based on (i) type of electrolyte, (ii) compatibility of electrolyte with the electrode material, (iii) the size of electrolyte ions and (iv) contacts between electrolyte and electrode material. As reviewed by Zhong et al. (2015), the electrolyte can be classified into liquid electrolyte comprising aqueous electrolyte (acid, alkaline and neutral) and non-aqueous electrolyte (organic electrolyte and ionic liquids), solid-state electrolyte (dry solid polymer electrolyte, gel polymer electrolyte and inorganic electrolyte) and redox active electrolyte (aqueous electrolyte, organic electrolyte, ionic liquid, and gel polymer electrolyte). Each electrolyte has its own advantages and disadvantages. For example, non-aqueous electrolytes have a wider cell operating potential window compared to aqueous electrolytes (Haas and Cairns, 1999). However, the aqueous electrolyte has greater specific capacitance and conductivity than non-aqueous electrolytes. Therefore, a careful selection of electrolyte is a must to obtain high performance supercapacitors. Another way to maximize the cell potential is by assembling asymmetrical supercapacitors. Asymmetrical supercapacitors with different positive and negative electrodes are able to extend the potential window compared to symmetrical assembly.

There is so much fascinating information on supercapacitors and a single review article is not enough to cover all of it. In the pursuit of producing high performing supercapacitors, a variety of materials have been explored. In light of this, conducting polymers, carbon-based materials and transition metal oxides/hydroxides are the most prospected electrode materials (Kulandaivalu et al., 2018; Mohd Abdah et al., 2018a,b). In recent times, the research is directed toward the development of composites to impede the demerits of these single constituents and to produce high-performance nanostructured materials. Over the last decades, we have seen tremendous improvement in the supercapacitors by designing new nanocomposite electrode materials. The attraction of electrode material for supercapacitor should be based on the following criteria:

a) low cost and easy to prepare.
b) high electronic conductivity to ease the ion transport within the electrode materials. Therefore, will increase the specific capacitance, specific energy, specific power and rate capability.
c) the high surface area with desirable pore size to increase the specific capacitance.
d) high mechanical and chemical stability to withstand the long charge-discharge cycles

The utilization of carbon-based materials in the fabrication of active materials for hybrid supercapacitors is a common practice. This is because of the versatility of carbon-based materials serve as a backbone due to their high mechanical strength, high hardness and excellent thermal properties. In most instances, carbonaceous materials often introduced with pseudocapacitive materials to enhance the supercapacitive performance, such as stability during charge-discharge cycles, the electrical conductivity of the composites and reduce the volume expansion of the composites. In recent years, metal hydroxides including layered double hydroxides (LDHs) have been explored widely as active materials for their multiple oxidation states. Herein, we highlight the advances in the investigation of LDHs containing Ni^{2+} and $Co^{2+/3+}$ with carbon-based materials as electrode materials for supercapacitors. There are several reviews on LDHs that disclose valuable insights on the LDHs and its related composites on their structures, preparation methods, applications and functionalities as summarized in **Table 1**. However, to the best of our knowledge, an extensive review of Ni-Co LDH/carbon nanocomposites for supercapacitors has not been previously reported. This review is intended to provide broad insight into the fundamental understanding of LDHs as well as Ni-Co LDH and Ni-Co LDH/carbon nanocomposites as electrode materials for supercapacitors.

LAYERED DOUBLE HYDROXIDES

LDHs are one of the most captivating 2D inorganic materials that have been applied in various fields, such as anticancer nanomedicine (Kim et al., 2018), photocatalysts (Shao et al., 2015), electrocatalysts (Long et al., 2014), and electrodes in energy storage and conversion technologies (Wang et al., 2018a; Kulandaivalu et al., 2019). The breakthrough of LDHs began with the amazing discovery of hydrotalcite minerals as synthetic materials in the 1940s by Feitknecht and Gerber (1942). However, when it was first described in 1842 by Hochstetter (1842), it was not widely acknowledged by the world as hydrotalcite but rather as mixed hydroxides, magnesium–aluminum hydroxycarbonate with the composition of $Mg_6Al_2(OH)_{16}CO_3{\cdot}4H_2O$. In addition, it is also the first natural occurring hydrotalcite reported in history. Yet, it was not until the 1960s after the discovery of hydrotalcite minerals that the detailed structure analysis on these minerals was fully outlined by Allmann and Taylor using the single crystal X-ray diffraction technique and identified it as the LDHs (Allmann, 1968; Taylor, 2018).

The LDHs are ionic lamellar compounds and better known as hydrotalcite-like clay materials. The name hydrotalcite is due to the similarities to the talc and high water content. Generally, the hydrotalcite-like clay materials can be classified into two types; cationic clays and anionic clays. The naturally occurring hydrotalcites are referred to as cationic clays. They have a stacking of negatively charged layers that have cations within the interlayer regions (**Figure 3**). The layers contain octahedral

TABLE 1 | The recent reviews on layered double hydroxide for supercapacitors.

Title	Summary	References
Research progress of Ni-Mn layered double hydroxide for supercapacitor	This review covers Ni-Mn LDHs as electrode materials for supercapacitors. A brief discussion on the synthesis method of Ni-Mn LDHs and the detailed research developments of Ni-Mn LDHs and its composites in asymmetrical supercapacitors were also discussed	Yan et al., 2018
Recent advances in layered double hydroxide as electrode materials for high-performance electrochemical energy storage devices	In this review, the author discussed the direct and indirect preparation method of various LDHs in detail. Adding to it, the authors also disclose the significant progress on the LDHs in electrochemical energy storage systems including supercapacitors and batteries	Sarfraz and Shakir, 2017
Layered double hydroxides toward high performance supercapacitor	In this review, the authors summarize the recent works of various LDHs as electrode materials for supercapacitors. Moreover, the composition adjustment of LDHs comprising the interlayer anions and host layer metal ions also discussed in detail	Li et al., 2017c
Chemical power source based on layered double hydroxides	The authors highlighted the recent progress of various LDHs in supercapacitors, fuel cells, metal-air batteries, lithium-ion batteries	Wang et al., 2015
Layered Double Hydroxide/Graphene Composites and Their Applications for Energy Storage and Conversion	The synthesis of LDHs/graphene-based composites was discussed in this article. Their performances in supercapacitors and electrochemical oxygen evolution reaction catalysis were also addressed	Hai-Yan Wang, 2018
Layered double hydroxide-graphene-based hierarchical nanocomposites: Synthetic strategies and promising applications in energy conversion and conservation	Methods in designing LDHs/graphene-based composites, and their applications as electrode materials in supercapacitors and as electrochemical or solar energy-driven photocatalytic water oxidation catalysts were addressed in detail	Varadwaj and Nyamori, 2016
Graphene/layered double hydroxides nanocomposites: review of recent progress in synthesis and application	This review covers the recent developments of LDHs/graphene-based composites along with their synthesis methods in various applications including oxygen evolution reaction, supercapacitors, hybrid sensors, adsorption, catalysis, water purification and flame retardant materials	Daud et al., 2016
Recent progress in layered double hydroxide based materials for electrochemical capacitors: Design, synthesis and performance	This review focuses on the broad aspect of LDHs and their composites with carbon materials, metals, metal oxides, metal sulfides, metal phosphides and polymers and further reviewing their performances for supercapacitors	Zhao et al., 2017

sheets in between the tetrahedral sheets, where typically cations in the tetrahedral sheets are silicon ion (Si^{4+}) and aluminum ion (Al^{3+}), whereas in octahedral are Al^{3+}, ferric ion (Fe^{3+}), and magnesium ion (Mg^{2+}) (Vaccari, 1998).

Unlike cationic clays, the anionic clays are commonly referred to LDHs that stacking brucite-like layers. Typically, the mirror image of cationic clays is the anionic clays. Instead of cations as in cationic clays, the anionic clays consist of anions in the positively charged interlayers (Abellán et al., 2020). In order to understand the structure of LDHs, the insights on the structure of brucite, $Mg(OH)_2$ is very crucial. In brucite, the hydroxyl ions are placed in the six vertices of the octahedral surrounding the divalent Mg^{2+} ion, which are located in the middle (**Figure 4A**). Each individual octahedral unit shares its edges with each other forming electrically neutral infinite layers. These layers are stacked one on top of another and bonded through hydrogen bonds, forming the brucite. The hydroxyl ions in these layers are closely packed giving 2D triangle symmetrical geometry. Then, the positive charges are introduced in the layers by partially replacing the Mg^{2+} ions with Al^{3+} forming the Mg-Al LDHs. The layers are then neutralized by the anions that intercalated in the interlayer region (in between the successive layers of layered double hydroxides). Water molecules also present in between the layers that bound with the hydroxide ions through hydrogen bonds (Sun et al., 2015). Various combinations of metal ions in LDHs also synthesized in a similar manner which can be expressed by the general formula:

$$[Me^{2+}{}_{1-\chi}Me^{3+}{}_{\chi}(OH)_2]^{\chi+}(A^{\alpha-})_{\chi/\alpha}.yH_2O$$

where, Me^{2+} is divalent metal cations (Zn^{2+}, Ni^{2+}, Co^{2+}, Ca^{2+}, etc.) and Me^{3+} is trivalent cations (Al^{3+}, $Cr^{3}+$, Fe^{3+} etc) as shown in **Figure 4A**. $A^{\alpha-}$ is abbreviated for anions with negative charges (Cl^-, CO_3^{2-}, NO_3^-, etc). A broad range of χ values have been reported in the preparation of LDHs, however, there is still disagreement is fixing the limit of the values. Nevertheless, in the preparation of pure LDHs, the χ values are fall in the range of $0.2 \leq \chi \leq 0.33$ (Walton, 2018).

The wide compositional and structural diversities in the LDHs system such as tunability of metal cations in the layers, easy adjustment of the molar ratio of metal cations and exchangeability of interlayer anions bestow various types of LDHs with unique architectures leading to incomparable physical and chemical properties. Adding to this, the variable oxidation states of metal cations in the LDHs and substitution of metal cations in the layers which provide high dispersion of metals boost the exploitation of metals cations of LDHs. Thus, these properties aid in enhancing the capacitive performances of LDHs as active materials particularly in supercapacitors as summarized in

Figure 4B. Indeed, over the last decades, there are ever-growing publications related to the LDHs as electrode materials for supercapacitors (**Figure 4C**).

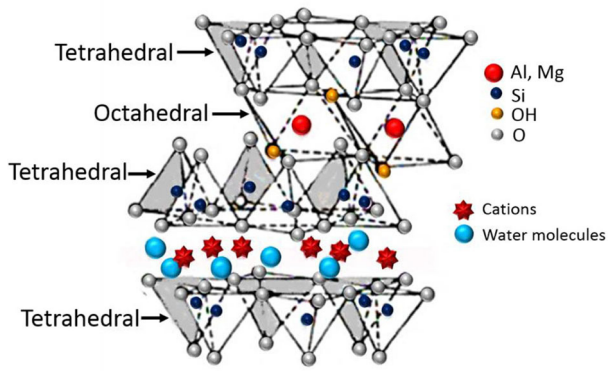

FIGURE 3 | Schematic illustration of cationic clay (Ghadiri et al., 2015).

STRUCTURAL IDENTIFICATION OF LDHs

One must be aware that X-ray diffraction (XRD) is a primary technique to analyze the crystalline phases, degree of crystallinity, and crystallite sizes of layered compounds (Cullity, 1957). Practically, in order to develop the layered compounds involving intercalation, knowledge on its crystalline structure is a must.

Prior to the XRD measurements, it is crucial to obtain a good Me^{2+}/Me^{3+} stoichiometry (the χ values) based on the molarity of species in LDHs. As mentioned earlier, the often reported χ values to fall between $0.2 \leq \chi \leq 0.33$, where the Me^{2+}/Me^{3+} ratio is between 2 and 4. The χ value is obtained using the following formula:

$$\chi = \frac{Me^{3+}}{Me^{3+} + Me^{2+}} \tag{3}$$

There are some arguments on the purity and structures of the compound formed if the χ values fall beyond the above-mentioned range. If the χ value is above 0.33, most likely Me^{3+}-O–Me^{3+} linkages will occur causing the electrostatic

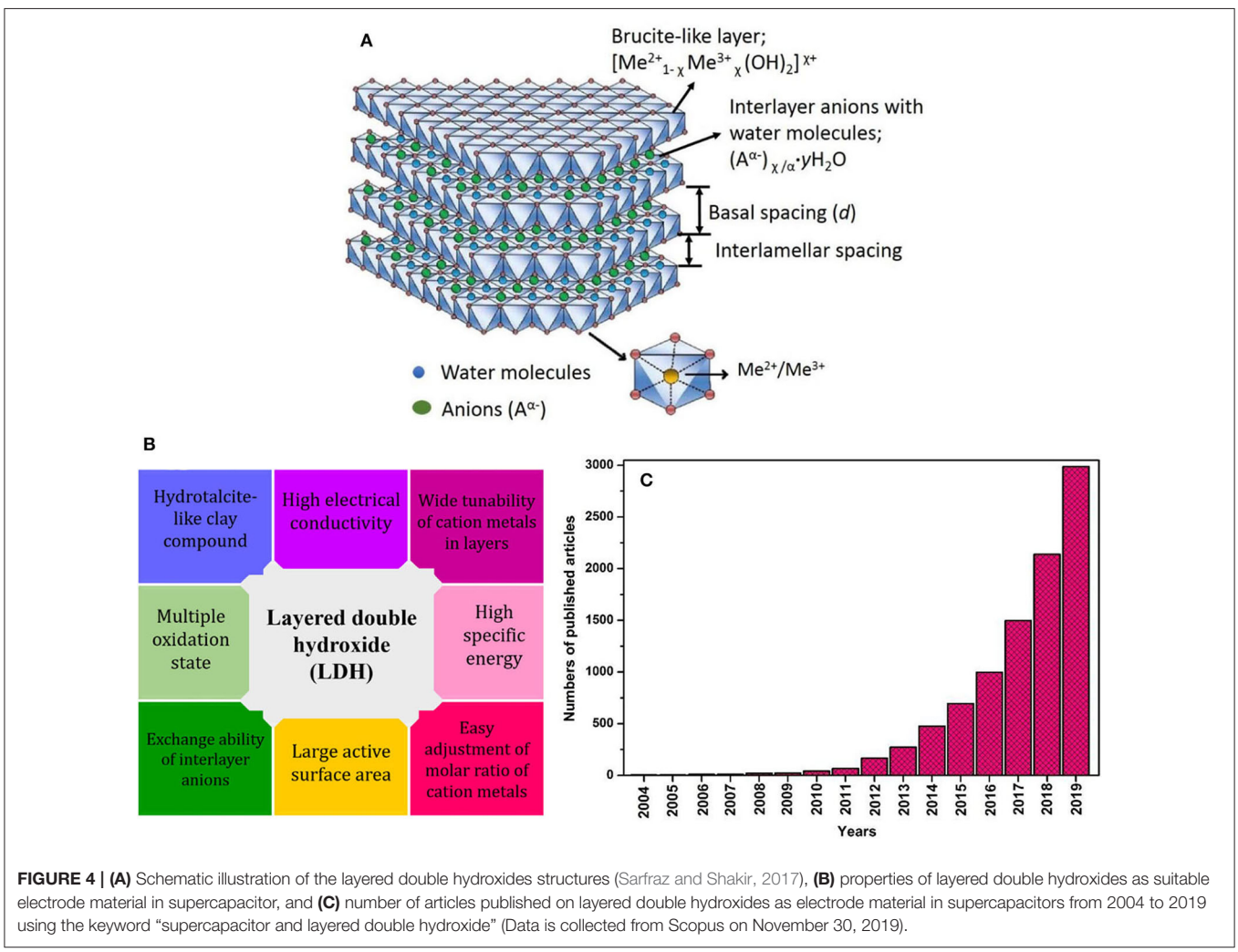

FIGURE 4 | (A) Schematic illustration of the layered double hydroxides structures (Sarfraz and Shakir, 2017), **(B)** properties of layered double hydroxides as suitable electrode material in supercapacitor, and **(C)** number of articles published on layered double hydroxides as electrode material in supercapacitors from 2004 to 2019 using the keyword "supercapacitor and layered double hydroxide" (Data is collected from Scopus on November 30, 2019).

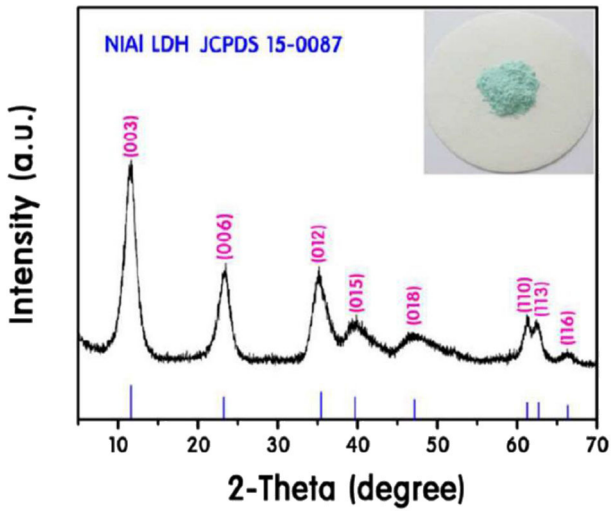

FIGURE 5 | XRD pattern of NiAl (Li et al., 2017a).

repulsion which eventually disturbs the lattice position. This phenomenon is termed as the cation avoidance rule. This rule defines from the secondary coordination sphere's point of view, where a 3+ metal cation could not contain another 3+ metal cation (Forano et al., 2006; Wang et al., 2013b). However, in a rare occurrence, χ values more than 0.33 are found, but it is believed this might be due to the experimental errors such as the presence of hydroxide compounds with amorphous phases that undetectable by the XRD or anions intercalated outside the hydrated layer galleries (Arias et al., 2013). On the other hand, if the $\chi < 0.33$ (which means Me^{2+}/Me^{3+} ratio is below 2) it will cause damages to the structure of LDHs due to the substitution of large Me^{3+} in LDHs (Wang et al., 2013b). Also, unusually very low or very high range of stoichiometry will result in the formation of LDHs with a mixture of other hydroxide compounds, $Me^{2+}(OH)_2$ or $Me^{2+}(OH)_3$ or $Me^{3+}OOH$ that provide inaccurate results. Therefore, stoichiometry is very important to produce pure LDHs.

The molar ratio of Me^{2+}/Me^{3+} is also equally important in the particle size of the resultant LDHs. LDHs prepared with a molar ratio between 1 and 3 provide a highly monodispersed particle size distribution (Chang et al., 2013). Yet, it is also expected that the LDHs might grow in disordered orientation when the molar ratio is approaching 1 (Cavani et al., 1991). Still, the root cause for the disordered phase could not be centered solely on the molar ratio. The preparation criteria, e.g., temperature, pressure, choice of precursors, and co-precipitation pH is also responsible for this formation (Pausch et al., 1986). However, when the molar ratio exceeds 3, noticeable enlargement in the particle size is normally observed due to agglomeration (Sun et al., 2015).

XRD is an important method in evaluating the LDHs formation. The confirmation of LDHs formation is accomplished by the presence of basal reflections (00*l*), at lower degrees ($2\theta = 10$ to 35°). The basal reflections indexed as (003) and (006) appear as strong/sharp, narrow and symmetrical diffraction peaks (**Figure 5**). These peaks designate to the basal reflection of intercalated anions (e.g., Cl^-, NO_3^-, SO_4^{2-}) in the galleries and ordered stacking sequence of LDHs (Mahjoubi et al., 2017; Richetta et al., 2018). Moreover, it is an indication of the formation of highly crystalline LDHs. The first basal reflection (003), more commonly appears with higher intensity than the second basal reflection, (006). However, in certain cases, the (006) reflection emerges more intense than the reflection of (003) which is related to the presence of complex metal anion in the interlayer of LDHs which increases the electron density in the midplane (Boclair et al., 1999; Beaudot et al., 2004).

The basal spacing is another important aspect of the LDHs and it can be calculated from the XRD pattern using the Bragg law:

$$n\lambda = 2d_{hkl}\sin\theta \tag{4}$$

where n is the diffraction order (an integer), λ is the wavelength of the X-rays (nm), d is the basal spacing (Å) and θ is the diffraction angle. Basal spacing is defined as the distance from the plane of a layer with its adjoining layer as shown in **Figure 4A**. The value of basal spacing is determined from the reflections of basal peaks (00*l)* and in some cases from the reflections of non-basal peaks ($hk \neq 0$). Of course, when preparing the LDHs, the basal spacing will arise differently depending on the preparation condition as mentioned earlier. Nevertheless, the molecular symmetry, charge, structure, size, type and orientations of anions used in the preparation of LDHs have a great influence on the basal spacing (Albiston et al., 1996; Kameda et al., 2006). Adding to this, intercalation and removal of water molecules into/from the interlayers also have an impact on the basal spacing (Li et al., 2017b).

Another essential step in analyzing the LDHs structure is determining the unit cell parameters. The basal spacing of reflection (003) defines unit cell parameter c or known as an interlayer distance along the c-axis and it represents the thickness of one brucite-like layer and one interlamellar space (Li et al., 2004). Note that, the c parameter would appear larger if there is a presence of impurities in the interlamellar space. Additionally, by assuming the thickness of the brucite-like layer to 4.769 Å as reported by Miyata (1975), the value interlamellar spacing can be deduced. Whereas, the basal spacing of reflection (110) defines the unit cell parameter a which reflecting the distance between the two metal cations within the layers. These values could be obtained using the expression, $c = 3d_{(003)}$ and $a = 2d_{(110)}$.

Ni-Co LAYERED DOUBLE HYDROXIDES

As it has been described earlier, redox active materials such as transition metal-based hydroxides and oxides have been used as active materials over a long period of time in supercapacitors due to their extraordinary properties such as high theoretical specific capacitance, multiple oxidation states and easy modification (Liu et al., 2018b; Qiu et al., 2018). Particularly, ruthenium oxides with high proton conductivity and high reversible oxidation-reduction process inevitably stand as a promising active material for supercapacitors. Nevertheless, this material is also known

for its high toxicity, high-priced and rareness in nature obstruct its wide applicability (Kim and Kim, 2006; Vellacheri et al., 2012). Apart from ruthenium oxides, nickel-based redox active materials and cobalt-based redox active materials are considered as promising active materials. In that context, to date, nickel hydroxides, $Ni(OH)_2$ and cobalt hydroxides, $Co(OH)_2$ are the most notably explored single metal hydroxides particularly in supercapacitors.

$Ni(OH)_2$ is extensively studied due to its low toxicity, abundance in nature, inexpensive and environmental friendliness. Nevertheless, it exhibits a low electrical conductivity ranges from 10^{-13} to 10^{-17} S cm^{-1} which consequently decreases the rate capability and life span (Motori et al., 1994). Moreover, slow ion diffusion rates and volume expansion during the charge-discharge cycles also restraining its electrochemical storage applications. α and β-$Ni(OH)_2$ have a high theoretical capacitance of 2,081 F g^{-1} within the potential window of 0.5 V (Wang et al., 2018c). α-$Ni(OH)_2$ is thermodynamically less stable than β-$Ni(OH)_2$ and easily converted to β-phase material by aging in alkaline solution or during continuous charge-discharge process. However, the former has a higher specific capacitance and good ionic conductivity than the latter due to high charge capacity and electrochemical reversibility (Meng and Deng, 2016). Additionally, despite the fact that both α-$Ni(OH)_2$ and β-$Ni(OH)_2$ contain close-stacked 2D $Ni(OH)_2$ layers, only α-$Ni(OH)_2$ comprises intercalated species (anions and water molecules). Thereby, resulting in differences in the electrochemical properties (Bastakoti et al., 2012).

$Co(OH)_2$ also possesses merits similar to $Ni(OH)_2$ such as low cost, environmental compatibility and high reversibility. $Co(OH)_2$ also exists in two polymorphs, α and β-$Co(OH)_2$. Compared to β-$Co(OH)_2$, α-$Co(OH)_2$ has higher electrochemical activity due to its larger interlayer spacing. The α-$Co(OH)_2$ with hydrotalcite structure is highly unstable structure and easily convert into brucite-like β-$Co(OH)_2$ (Cui et al., 2013). Additionally, this single hydroxide material also has a high theoretical capacitance of ∼3,460 F g^{-1} in a potential window of 0.6 V (Cao et al., 2004).

Undoubtedly, both of these materials exhibit exceptional properties. The great feasibility of these layered materials with large interlayer spacing endows effective accommodation of ions from the electrolyte in interlayers (Cui et al., 2013). Hence, the specific capacitance and rate capability can be enhanced significantly. Therefore, by combining these materials in the formation of Ni-Co LDHs can improve the overall performances in supercapacitors in terms of specific capacitance, cycling stability and rate capability. Incorporating nickel into the $Co(OH)_2$ system and vice versa gains benefits from the other and overcomes the drawbacks. The presence of nickel help in strengthening the electrochemical performances, while cobalt increases the electrical conductivity of the LDHs system (Windisch et al., 2001). It is reported that the formation of γ-NiOOH from $Ni(OH)_2$ is responsible for the volume expansion. Therefore, by incorporating cobalt into the $Ni(OH)_2$ the formation of γ-NiOOH can be surpassed as it can improve the oxygen over potential. While, during the charge-discharge process, the oxidation of Co^{2+} to highly conductive CoOOH improves the overall conductivity of the electrode material (Chen et al., 1999).

The performance of Ni-Co LDHs depends on the faradaic redox reaction of cobalt and nickel hydroxides. The charge storage of Ni-Co LDHs is related to chemical state changes of Ni^{2+}/Ni^{3+} and $Co^{2+}/Co^{3+}/Co^{4+}$, which refers to the adsorption of ions onto the surface of active materials during the redox reaction. The charge storage mechanism of Ni-Co LDHs during electrochemical measurements in the aqueous electrolyte is shown in the Equations 3–5 (Xie et al., 2012):

$$Ni(OH)_2 + OH^- \rightarrow NiOOH + H_2O + e^- \quad (5)$$

$$Co(OH)_2 + OH^- \rightarrow CoOOH + H_2O + e^- \quad (6)$$

$$CoOOH + OH^- \rightarrow CoO_2 + H_2O + e^- \quad (7)$$

FACTORS INFLUENCING THE FORMATION OF Ni-Co LDHS

Ni-Co LDHs have been an ideal candidate for supercapacitors for their distinctive layered structures, flexible tunability of anions/cations, and multiple oxidation states. In recent years, researchers have done astounding works on Ni-Co LDHs and they have focussed mainly on the composition, morphology, particle size and surface area of the LDHs in order to obtain high performance materials. It should be noted that the effectiveness of the charge storage of Ni-Co LDHs in supercapacitor varies with the properties of this active material. Morphologies, crystallinity, electrical conductivity and surface area of LDHs are very important to determine the electrochemical performances. Therefore, the factors influencing these factors will be reviewed in this section.

pH

Among the different fabrication routes for the LDHs, the co-precipitation method at a constant pH is commonly used. The pH value has a pivotal role in the formation of LDHs, particularly on the structure of LDHs. Typically, an alkaline solution (precipitant) added into the mixed metal salt solution to control the pH at a selected value has resulted in the co-precipitation of metals. Various type of alkaline solution is utilized to control the pH. With regard to Ni-Co LDHs, Li et al. (2016c) and Wang et al. (2018b) have chosen pH 8 as the optimal value to prepare the Ni-Co LDHs. Whereas, Cheng et al. (2013) and Mehrabimatin et al. (2019) have synthesized the LDHs by adjusting the pH at 9 through the addition of ammonium hydroxide solution. While, Shen et al. (2019) have used sodium hydroxide to maintain the pH to 9. On the contrary, pH 10 was also reported as the optimum medium to prepare the Ni-Co LDHs (Cao et al., 2019). In this study, the author used L-ascorbic acid and ammonia to control the pH. The precipitation pH value of 7.34 has also been reported using 2-methylimidazole (Wang et al., 2017b). The rule of thumb in this whole synthesis process is the pH value should exceed 4.0 and the pH range from 7 to 10 is commonly used to synthesize the Ni-Co LDHs. This is due to the fact that in the acidic condition the brucite-like layer in the LDHs will collapse. It also greatly argued that at lower pH

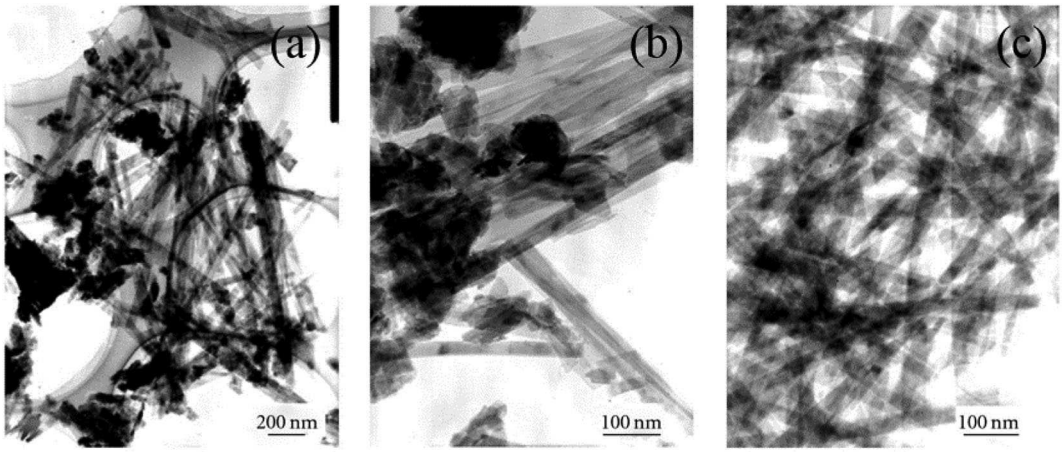

FIGURE 6 | TEM images for Ni/Al LDHs synthesized at different pH values. **(a)** 5.5, **(b)** 8.5, **(c)** 10.0 (Zhao et al., 2011).

values, an amorphous compound is produced, while at higher pH values, the brucite-like layer of LDHs with high crystallinity will evolve. However, there is no extensive works have been carried out to prove this statement. Furthermore, the addition of precipitant in the synthesis of LDHs produces hydroxide ions which involve in the redox reaction and eventually increase the crystallinity and hydrophilicity of the LDHs (Wang et al., 2013a). Thus, the charge transport and ion movement will be reinforced. Additionally, the basic growth condition also encourages the fast and uniform growth of LDHs whether in the form of nanoparticles or flower-like structure or flakes-like morphologies (Wang et al., 2013a). Talking about morphology, pH has a great impact on the morphology of LDHs which indirectly reflects the surface area (**Figure 6**). One must notice that different pH values resulted in different morphologies, such as nanorods, nanosheets, 3D nanoparticles, etc. (Zhao et al., 2011; Li et al., 2016c). However, there are little references which have been reported on the effect of pH on the morphology of Ni-Co LDHs. Nevertheless, the selection of pH for the formation of LDHs should be suitable for both metal ions (in the case of LDHs with two types of metals) to precipitate simultaneously. Therefore, it is always preferred to choose a pH value higher or equal to the precipitation pH value of a respective metal hydroxide considering their solubility equilibrium constants. In contrast with the usual basic condition, a study reported pH 6, as the optimal pH to prepare the Ni-Co LDHs using electrodeposition method (Chen et al., 2014c). The author claimed that at pH $\geq$ 7, pre-precipitation of hydroxides occurs causing higher rate of $Co(OH)_2$ formation than LDHs due to its low solubility at this pH. Whereas, at pH 6, the rate of nickel and cobalt hydroxides formation in LDHs is equal. Adding to this, a significant variation in values of specific capacitance is also noted when the pH is varied. When deciding the value of pH for LDHs synthesis, a fair consideration need to place on the type and nature of anions of the LDHs. This is due to the solubility of anions (e.g., Cl^-, NO_3^-, SO_4^{2-}) which differ from each other. Therefore, the amount of anions intercalated in the LDHs and the size of LDHs nanoparticles are also vary (Li et al., 2010). Moreover, the stability of LDHs is determined by the stability of intercalated anions. For example, Ni-Co LDHs containing chloride anion in the interlayer are stable in the pH ranging from 3.8 to 8.9 (Sun et al., 2013).

In general, Ni-Co LDHs can be synthesized in basic aqueous solution and mild acidic or near a neutral aqueous solution. Nevertheless, the selection of pH is not solely relied on one particular factor but other criteria for instance concentration of metals salts, the ratio of Me^{2+}/Me^{3+} ions, type of anions and preparation method which need to be taken into consideration.

Ratio

The optimization of the Me^{2+}/Me^{3+} ratio in LDHs is pivotal in the morphology, phase structure and capacitive behavior. Pointing to Ni-Co LDHs, plenty of work has been performed on the optimization of Ni^{2+}/Co^{2+} ratio (Wang et al., 2017b, 2019a). Synthesizing the Ni-Co LDHs by varying the metal ion ratios may result in variation in growth rates, nanostructures and pore size/size distribution (**Table 2**). Sun et al. (2013) studied the changes in the structure of Ni-Co LDHs when the metal ion ratios are altered. From the morphological point of view, when the ratio of cobalt is increased with respect to nickel (Ni:Co), changes from flower-like nanosheets (1:0) to nanosheets (1:1), nanospheres enclosed in nanoplates (1:2), highly porous 1D nanorods (1:4) and nanoparticles (0:1) is noticed. Interestingly, the Ni-Co LDHs (1:4) with 1D nanorods exhibited excellent electrochemical performances regardless of their average specific surface area than the ratio of 1:2. It was deduced that the broad pore size distribution (2 to 15 nm) in the former sample compared with other metal ratios reduces the charge transfer resistance and promotes the movement of electrolyte. In contrast with this finding, Kulkarni et al. (2013) demonstrated nanoflakes morphology for all Ni-Co LDHs (1:0, 0.75:0.25, 0.5:0.5, 0.4:0.6, 0.25:0.75, and 0:1), however, they showed variation in flakes size, pore size/distribution and the number of layers. The authors claimed that the amount of nickel in the layer is the

TABLE 2 | Summary of preparation condition, morphology, and specific capacitance of Ni-Co LDHs as supercapacitor electrode.

Method	pH	Ni/Co ratio	Temperature (°C)/ Reaction time (hour)	Capacitance	Nanostructure	References
Solvothermal	7.34	1:1	120/14	2,242.9 F g^{-1} at 1 A g^{-1}	Nanosheets	Wang et al., 2017b
Solvothermal	–	2:3	160/6	2,158.7 F g^{-1} at 1 A g^{-1}	3D hydrangea-like microspheres	Yan et al., 2015
Hydrothermal	–	2:1	100/10	293.9 C g^{-1} at 1 mA cm^{-1}	Nanowires	Zhang et al., 2019
Hydrothermal	–	9:1	100/48	808.4 C g^{-1} at 1 A g^{-1}	3D sea urchin-like nanosheets	Hou et al., 2019
Co-precipitation	8.72	6:4	55/15	2,228 F g^{-1} at 1 A g^{-1}	3D flower-like nanosheets	Li et al., 2016c
Electrodeposition	–	1:1	–	~0.8 F cm^{-2} at 2 mA cm^{-2}	Nanosheets	Wang et al., 2019c
Microwave-assisted hydrothermal	–	3:2	200/2	1,720 F g^{-1} at 3 A g^{-1}	Flower-like nanosheets	Wang et al., 2019b
i) Hot-air oven ii) Electrodeposition	–	2:1	90/9	536.96 μAh cm^{-2} at 2 mA cm^{-2}	Nanosheets on nanoflakes	Nagaraju et al., 2017
Co-precipitation	–	1:1	140/24	777 C g^{-1} at 1 A g^{-1}	Flower-like nanosheets	Qin et al., 2019
Hydrothermal	–	2:1	High temperature/2.5	–	Nanoflower	Wu et al., 2019b
Electrodeposition	–	4:1	–	374.7 mAh g^{-1} at 2 A g^{-1}	Nanosheets	Wu et al., 2019a
Co-precipitation	9	1:1	–	2,305 F g^{-1} at 1 A g^{-1}	Nanodisc	Cheng et al., 2013
Electrodeposition	–	1:1	–	2,200 F g^{-1} at 5 A g^{-1}	Nanotubes with nanosheets	Liu et al., 2017
Electrodeposition	–	2:1	–	1,862.4 F g^{-1} at 4 A g^{-1}	Nanosheets	Nagaraju et al., 2016
Microwave-assisted hydrothermal	–	1:1	100–140/1–3	1,580 F g^{-1} at 10 A g^{-1}	Nanocones	Liu et al., 2012
Electrodeposition	–	1:1.5	–	2,104 F g^{-1} at 1 A g^{-1}	Nanosheets	Gupta et al., 2008
Co-precipitation	–	1:4	80/6	1,030 F g^{-1} at 3 A g^{-1}	1D nanorod	Sun et al., 2013
Electrodeposition	–	1:1	–	~1,300 F g^{-1} at 1 A g^{-1}	Nanoflakes	Ge et al., 2019
Electrodeposition	–	1;2	–	~1,213 F g^{-1} at 5 mV s^{-1}	Nanoflakes	Kulkarni et al., 2013
Electrodeposition	–	1:2	–	1.536 C cm^{-2} at 2 mA cm^{-2}	Flower-like nanosheets	Yang and Li, 2019
Electrodeposition	–	1:2	–	1,200 F g^{-1} at 1 A g^{-1}	Nanosheets on nanorods	Wen et al., 2016
Solvothermal	–	1.5:1	180/24	~900 F g^{-1} at 1 A g^{-1}	Nanosheets	Cai et al., 2015
Co-precipitation	–	1:2	Room temperature/6	~550 F g^{-1} at 2 A g^{-1}	Flower-like nanosheets	Zhao et al., 2015
Electrodeposition	–	1:2	–	1.52 C cm^{-2} at 2 mA cm^{-2}	Open porous nanosheets	Nguyen et al., 2017
Hydrothermal	–	1:1	100/10	1,734 F g^{-1} at 6 A g^{-1}	Nanosheets	Pu et al., 2014
Hydrothermal	–	1:1	160/6	1,600 F g^{-1} at 1 A g^{-1}	Interconnected nanosheets	Xia et al., 2015
Co-precipitation	9	1:1	Room temperature/12	1,809 F g^{-1} at 1 A g^{-1}	Flower-like nanosheets	Hu et al., 2009
Electrodeposition	–	2:1	–	1,587.5 F g^{-1} at 0.5 A g^{-1}	Nanosheets	Wei et al., 2018
Microwave-assisted hydrothermal	–	4:1	–	1,170 F g^{-1} at 4 A g^{-1}	Hexagonal nanosheet	Chen et al., 2014a
Co-precipitation	–	2:1	–	774 F g^{-1} at 0.2 A g^{-1}	Hexagonal crimpled nanosheet	Wang et al., 2016
Hydrothermal		3:7	110/0.5	943 F g^{-1} at 20 mV s^{-1}	Interwoven fabric	Jeong et al., 2019
Hydrothermal co-deposition		1.5:1	180/24	2,682 F g^{-1} at 3 A g^{-1}	Porous nanostructure	Chen et al., 2014b

deciding factor for the morphology of LDHs. They support their arguments with a wettability study where the LDHs with high nickel contents showed superhydrophilic characteristics. Regardless of the detailed explanation given in this study, the authors missed to address the importance of cobalt in the LDHs, and how does it influence the morphology of LDHs.

The metal ion ratios also influence the crystallinity and phases of LDHs. Sun et al. (2013) have studied that when Ni-Co ratio (which varies from 0 to 1) was lowered than 0.5, mixed phases of nickel hydroxide hydrate and cobalt carbonate hydroxide were more obvious in the LDHs. Moreover, the XRD peak intensities also weaken with the decrement of nickel to cobalt ratio exhibiting the poor crystallinity of LDHs. In another study on Ni-Co metal ion ratios of 0, 0.3, 0.6,1, 3 and 1 revealed contrary crystallinity results (Kulkarni et al., 2013), in which decrease of metal ion ratios leads to sharp and intense peaks of hydrotalcite phase, showing the good crystallinity of the LDHs.

Reaction Temperature

Unlike the carbon-based materials which are very stable in any temperatures, LDHs are very delicate and sensitive, making the selection of temperature in the synthesis of LDHs is very crucial. There is no fixed value of temperature for the formation of LDHs. The selection of temperature varies with a few factors namely synthesis method, aging time, type of metal cation and metal cation ratio etc. In most cases, even the same synthesis method was applied, and different temperatures was used. For instance, Hu et al. (2009) and Zhao et al. (2015) have prepared Ni-Co LDHs with flower-like nanosheets via co-precipitation method at room temperature. While, a few other studies reported similar findings at a temperature of 55°C (Li et al., 2016c) and

140°C (Qin et al., 2019) using the same method. The selection of temperature also depends on methods. Mostly, solvothermal and hydrothermal methods use higher reaction temperatures compared to the co-precipitation method. In the formation of LDHs, former methods are more preferable due to uniform and homogenous particle size compared to co-precipitation. Moreover, these methods produced LDHs with larger particle size with high crystallinity. The reason is that the reactants are exposed to thermal treatment at pressurized conditions. In a study conducted by Oh et al. (2002), the author reported that increasing the reaction temperature in the range of 100 to 180°C via hydrothermal method yielded LDHs with a larger particle size varying from 115 to 350 nm. The authors have also manifested that differences in the temperature have profound effect on the crystallinity of the LDHs as shown by the reflection intensity in the XRD. However, it is worth to note that at high temperature (> 300°C), the structure of LDHs tend to collapse (Li et al., 2012a).

CARBON MATERIALS

In the past decades, carbon materials are designed with LDHs to deliver high specific capacitance, specific energy, specific power and remarkable stability. Looking into the history, the word "carbon" is originated from the Latin word "*Carbo*" defining coal is now taking the world by storm. Carbon is found abundantly on the earth and almost all the living and non-living things on earth are made up of carbon. In the scientific world, carbon has been the most captivating material since the introduction of graphite and diamond; the allotropes to the world. Basically, it consists only of carbon atoms, but they have intriguing physical and chemical properties due to its remarkable electronic structures to adapt *sp*, sp^2, and sp^3 configurations. There are other several carbon allotropes such as fullerenes, carbon quantum dots, onion-like carbon, graphene-family nanomaterials (GFN), and so forth. The existence of carbon materials in different dimensional and forms made it stand out from other materials.

Generally, carbon materials can be classified according to their dimensionality; zero-dimensional (0D), one-dimensional (1D), two-dimensional (2D), and three-dimensional (3D) nanostructured materials. These materials have their unique characteristics that distinguish them from one to another. Briefly, the 0D carbon nanostructures are defined as particles with spherical-like shapes and their sizes are normally in nanometric range. The 0D nanostructured can be further classified into solid, hollow and core-shell nanostructured. The solid 0D carbon nanostructures (e.g., porous carbon) are famous for their variety pore size distributions; macroporous (>50 nm), mesoporous (2–50 nm), and microporous (<2 nm) materials. On the other hand, the volume density and high surface area-to-volume ratio are the merits of the hollow 0D nanostructures (Lai et al., 2012). Additionally, by controlling the inner and outer diameter, the features of the hollow shell such as thickness and surface porosity can also be tailored according to the needs. Whereas, the uniqueness of core-shell lies in the versatility of the core-shell which can be made of different materials as core or shell and tunability of the properties by varying the shape, size, morphologies and constituent of core-shell. The core-shell 0D carbon nanostructures are often referred to as a spherical-shaped core carbon coated with a carbon shell. The core-shells can also be fabricated in the form of mesoporous nanostructures. It is also feasible to fabricate carbon nanostructures with multiple particles of core coated with a sole shell or vice versa. A hollow carbon shell with a hollow core or with a removable core is another form of core-shell nanostructures (Feng et al., 2018). Fullerenes, onion-like carbon, carbon quantum dots, graphene quantum dots, and carbon nanoparticles are examples of 0D carbon nanostructures.

Whereas, fibers or wire-like shaped nanostructures are categorized as 1D carbon materials such as carbon nanotubes, carbon nanohorns, carbon nanofibers, carbon nanowires and so forth. The 1D carbon nanostructures have a high surface area-to-volume ratio and two-dimension restraints that give superior chemical and physical properties (Weng et al., 2014). Additionally, due to their unique geometrics, the 1D carbon nanostructures have remarkable electron and ion transport pathways. This will promote better electrochemical properties and the ability to endure the volume changes and adapts to the mechanical strain. The 1D nanostructures can be assorted into three groups; (a) relative ratio between length-to-diameter is < 10 (e.g., carbon nanorods), (b) relative ratio between length-to-diameter is more than 10 (e.g., carbon nanowires) (Li et al., 2019b) and (c) structure with hollow walls (e.g., carbon nanotubes) (Pan et al., 2018).

The 2D carbon nanostructures are defined as materials with two dimensions beyond the nanometric ranges (Tiwari et al., 2012). Interestingly, the 2D materials are in a layered shape resembling a planar sheet. The GFN including graphene, few-layered graphene (FLG), graphene oxide (GO) and reduced graphene oxide (rGO) are examples of 2D carbon nanostructures. These materials are known for their extraordinary conductivity and mechanical strength making them a suitable candidate for supercapacitors. For supercapacitor applications, the higher surface area to volume ratio makes GFN the most desirable materials. As an outstanding electrode, GFN predominantly graphene has a remarkably high theoretical surface area up to > 2,500 m^2/g (Singh, 2016). Yet, a propensity for self-agglomeration due to the existence of strong van der Waal forces between the graphene sheets is the main hurdle to generate graphene-based electrodes (Wang and Liu, 2011). The 2D graphene is the building block for 3D graphite. Basically, the 3D carbon nanostructures are made of low-dimensional building blocks and carbon foam and mesoporous carbon are the most explored 3D nanostructures. They have a high surface area and large electrode-electrolyte interface which provides efficient ion pathways (Tiwari et al., 2012; Zhi et al., 2013) as supercapacitor electrodes. Other than foams and mesoporous materials, activated carbon, carbon aerogels, nanopillars, nanoflowers, and nanocoils are also under the category of 3D nanostructures.

Even though the above-mentioned carbon materials possess fascinating properties, it is still a challenging endeavor for researchers to produce high-performance carbon materials as electrodes for supercapacitors. The collaboration of carbon materials with pseudocapacitive materials is a route to augment

TABLE 3 | Comparison of carbon materials, LDHs and carbon-LDHs composites as electrode materials for supercapacitors.

Materials	Specific capacitance	Conductivity	Surface area	Stability	Cost
Carbon materials	Low	Low	High	High	Cheap
LDHs	High	High	Moderate	Low	Expensive
Carbon-LDHs composite	Can be improved significantly depending on the suitable composition of the LDHs and carbon materials in the composite				Moderate

the electrochemical properties for supercapacitors. In this article, we will focus on the carbon materials combined with LDHs as electrode materials for supercapacitors and **Table 3** compares the properties of carbon materials, LDHs and carbon-LDHs composites as electrode materials for supercapacitors.

Ni-Based LDHS Combining With Carbon-Based Materials

In this section, Ni-based LDHs composite combined with carbon materials as electrodes for supercapacitors will be discussed. Li et al. (2015a) *in-situ* grown Ni-Al LDHs nanosheets on the carbon nanotubes pre-coated by the alumina (γ-Al_2O_3) showed decent improvement in term of capacitive performances. The use of γ-Al_2O_3 is very crucial in this study as a source of Al for the formation of LDHs. γ-Al_2O_3 has better dissolution than commonly used AlOOH (Li et al., 2012b). The author studied the asymmetrical configuration of this composite with activated carbon as the negative electrode and discovered a specific capacitance of 115 F g^{-1} with a specific energy of 52 Wh kg^{-1} at a current density of 1 A g^{-1}. He deduced that the introduction of carbon nanotubes is responsible for the exquisite performances shown by this composite, where carbon nanotubes (i) hinder the restacking of LDHs during synthesis, (ii) bridge the interfacial contact, and (iii) provide a conductive surface for uniform growth of nanosheets.

While, Li et al. (2014) have developed Ni-Al LDHs/rGO composite and compared the electrochemical performance of the same composite that reduced thermally and reduced via microwave irradiation. It has been shown that the former has the highest specific capacitance of 1,208 F g^{-1} at 8 A g^{-1} and able to retain the value to 1,518 F g^{-1} at 1 A g^{-1} (about 80%). The thermal treatment is responsible for creating pores for the ion movement to the interior of the composite. This highly porous composite also displayed an excellent life cycle with above 80% over 2,000 cycles. Another similar work has been reported by Yulian et al. (2013), where Ni-Al LDHs nanoflakes anchored *in-situ* on activated graphene nanosheets. This hybrid composite has a BET surface area of 3,026 m^2 $g^{-}1$ and showed a maximum specific capacitance of 1,173 F g^{-1} at a current density of 1 F g^{-1}. Gao et al. (2011) have also fabricated Ni-Al LDHs/graphene nanosheets via the hydrothermal method. The obtained composite displayed a high specific capacitance of 781.5 F g^{-1} at 5 mV s^{-1} and excellent cycling retention in a three-electrode configuration. While, Yang et al. (2013) have included graphene nanosheets and carbon nanotubes with Ni-Al LDHs via one-step ethanol solvothermal method. The obtained 3D flower-like composite was able to overcome the limitations of 2D graphene nanosheets i.e. aggregation, low surface area and deteriorations of ion movements. In this study, the role of graphene nanosheets was expected to be as a conductive scaffold to build a 3D nanostructure. More importantly, the composite revealed to possess 1,869 F g^{-1} at 1 A g^{-1} with superior cycling stability over 1,000 cycles.

Comparative study on sandwich-like Ni-Mn LDHs/rGO, Ni-Mn LDHs/carbon black, turbostratic-structured Ni-Mn LDHs/carbon nantotubes and ternary Ni-Mn LDHs/carbon nanotubes/rGO (**Figure 7**) were carried out by Li et al. (2016b). Electrochemical study in 2 M KOH revealed ternary Ni-Mn LDHs/carbon nanotubes/rGO has higher specific capacitance (1,268 F g^{-1} at 1 A g^{-1}) and superior cycle life (79% over 2,000 cycles) than other hybrid composites. This is due to the addition of rGO and carbon nanotubes where, (i) LDHs anchored firmly on the rGO, thus preventing restacking of LDHs nanosheets, (ii) carbon nanotubes provides conductive scaffold, hence increasing the conductivity of the composite, and (iii) the co-dispersed carbon nanotubes and rGO open a conductive network pathway for the ions.

Co-based LDHs Combining With Carbon-Based Materials

Great efforts have been committed to study Co-based LDHs composite combined with carbon materials as electrodes for supercapacitors. For example, honeycomb-like Co-Fe LDHs were *in-situ* deposited on the multi-layer graphene to be for energy storage devices. They showed a high specific capacitance of 882.5 F g^{-1} at 1 A g^{-1}. However, the composite only able to withstand 39% of its initial capacitance value over 2,000 cycles due to the detachment and dissolution of active material during the charge-discharge process (Xu et al., 2018).

Co-Al LDHs have also found its potential in energy storage applications. The Co-Al LDHs/rGO composite was prepared by the co-precipitation method, which formed nanosheets grown perpendicularly on the rGO layer. The composite has lesser agglomeration compared to pure LDHs with serious agglomeration (**Figures 8a,b**). The BET surface area was found to be 47.6 m^2 g^{-1} compared to that pure LDHs (24.0 m^2 g^{-1}) (**Figures 8c,d**). In an asymmetrical configuration, this composite as the positive electrode and activated carbon as the negative electrode was able to operate at a wide potential window (0 to 1.75 V), which results in enhanced specific energy (35.5 Wh kg^{-1}) and specific power (8.75 W kg^{-1}) (**Figure 8**e). Moreover, the asymmetrical assembly displayed excellent capacitance (90% retention) after 6,000 cycles (**Figure 8f**) (Zhang et al., 2013).

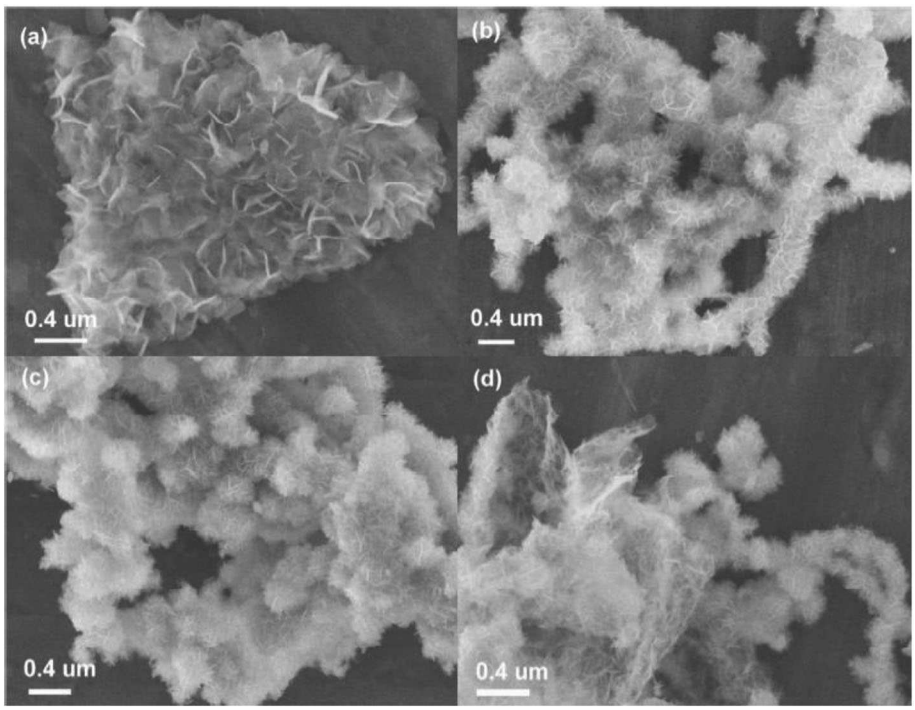

FIGURE 7 | SEM images of **(a)** Ni-Mn LDHs/rGO, **(b)** Ni-Mn LDHs/carbon nanotubes, **(c)** Ni-Mn LDHs/carbon black, and **(d)** Ni-Mn LDHs/carbon nanotubes/rGO (Li et al., 2016b).

In another study, Zhang et al. (2012) have demonstrated for the first time the fabrication of graphene nanosheets combined with Co-Al LDHs using the one-pot refluxing method. A 3D conductive network made of hexagonal flakes can be observed for this composite. The hexagonal flakes of Co-Al LDHs are covered on the surface of graphene nanosheets, preventing the re-stacking of graphene and giving rise to the surface area (23.4 m^2 $g–^1$) of the composite.

Ni-Co LDHs Combining With Carbon-Based Materials

Despite the endless effort of researchers to produce high performance Ni-Co LDHs electrode material with controlled morphologies, optimized particle sizes, enhanced surface area and broad pore size distribution, the main drawbacks including poor stability and low electrical conductivity have a profound effect on its practicability. In light of this, fabrication of composite materials, specifically the introduction of carbonaceous materials with Ni-Co LDHs could provide the right solution for this conundrum. The uniqueness and significant benefits of this combination are listed as follows (Xu et al., 2006; Li et al., 2016a; Wang et al., 2018a):

a) The severe aggregation of Ni-Co LDHs can be avoided. The charged surface of LDHs often aggregates by forming particles or irregular clusters with size ranges from 1 to 10 μm, thereby resulted in an unstable colloidal solution, which causes a serious impact on its electrochemical performances.
b) The electrical conductivity of the composite can be improved significantly by preventing the agglomeration of LDHs. Thus, electron transfer and rate of diffusion during the oxidation-reduction process will be facilitated.
c) Carbon-based materials provide large ion accessible surface areas with enhanced active sites facilitating efficient access of ions from the electrolytes and eventually shorten the ion diffusion pathway.
d) Importantly, the mechanical stability of the composite will be improved significantly. As known to all, carbon-based materials have extraordinary mechanical stability. In this instance, carbon-based materials will act as a backbone or scaffold to minimize the volume expansion of LDHs.

Thus, the introduction of carbon-based materials with Ni-Co LDHs have a considerable impact on the electrochemical performances of the composite. The studies conducted on the Ni-Co LDHs with carbon-based materials are quite encouraging (**Table 4**).

Most of the materials from carbon-based materials exhibit high surface area and good electrical conductivity. Due to these features, Ni-Co LDHs often introduced with graphene-based materials to improve the electrochemical properties of the composites. For example, Wang et al. (2019a) have directly fabricated Ni-Co LDHs/rGO grown on carbon cloth (CC) using a simple one-pot hydrothermal method. The Ni-Co LDHs uniformly grow on the CC forming hydrangea petal-like structure with 2D sheet-like morphology. While the rGO grew between the LDHs sheets were greatly improved the specific surface area of the composite. It was used directly as a binder-free electrode in a symmetrical supercapacitor. The as-prepared composite obtained specific capacitance of 151.46 F

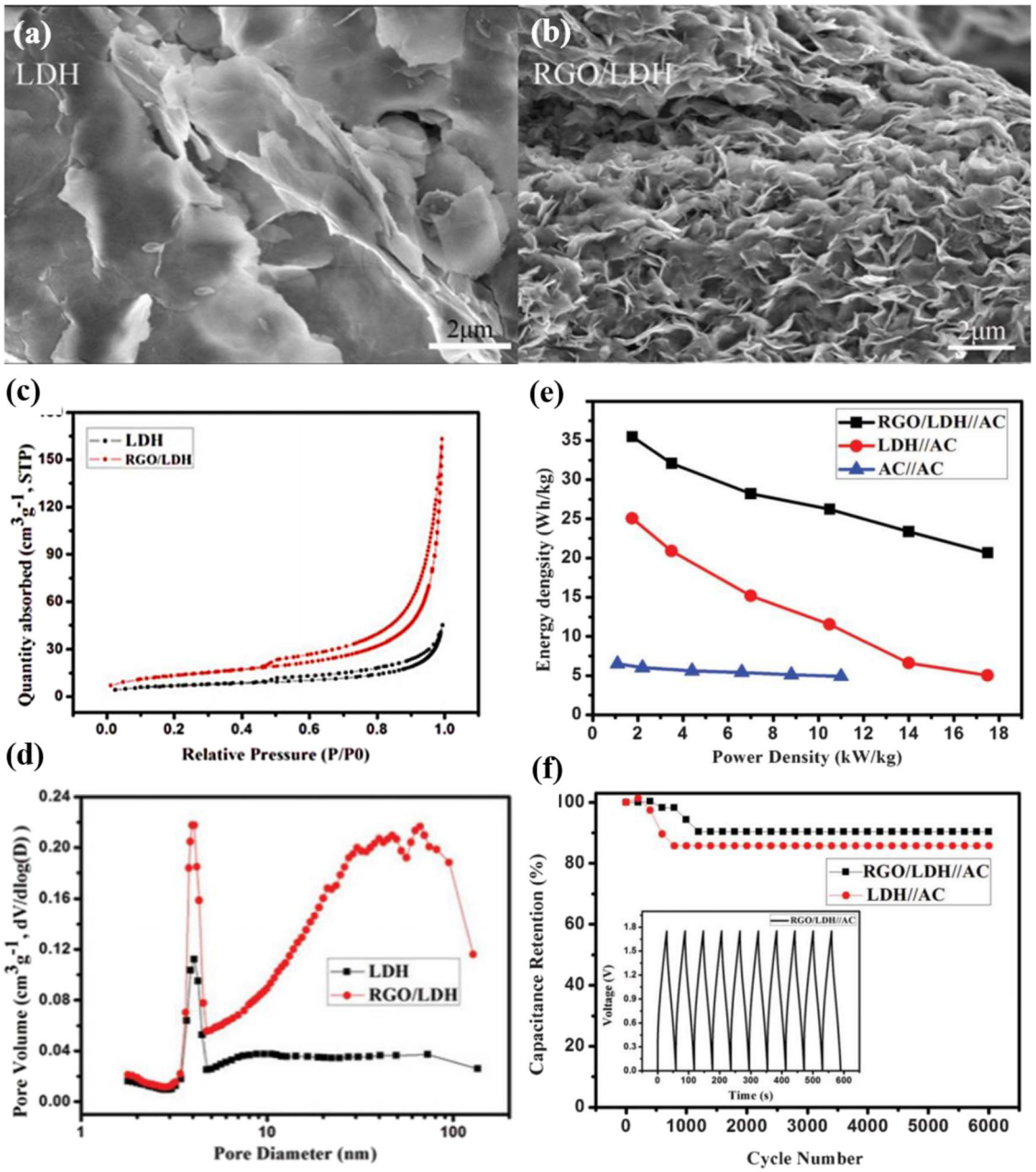

FIGURE 8 | SEM images of **(a)** LDHs, **(b)** low-magnification of rGO/LDHs, **(c)** nitrogen adsorption and desorption isotherm loops of LDHs and rGO/LDHs composite, **(d)** pore size distribution of LDHs and rGO/LDHs, **(e)** Ragone plots of LDHs//AC, rGO/LDHs//AC asymmetric ECs, and AC//AC symmetric EC, and **(f)** Cycle stability of LDHs//AC and rGO/LDHs//AC ECs during charge–discharge test at a current density of 4 A g^{-1} (Zhang et al., 2013).

g^{-1} at a current density of 2.5 A g^{-1} and prominent cycling stability of 85.6% after 3,000 cycles at 5 A g^{-1}. The author claimed that the hydrangea petal-like morphology of the Ni-Co LDHs/rGO/CC with large interlayer spacing facilitates the transport of ions between the composite and electrolyte and shorten the ion diffusion pathway endowing the electrode with a specific energy of 30.29 Wh kg^{-1} at a specific power of 1,500 W kg^{-1}. Importantly, after the continuous 3,000 cycling process, the structure of the composite does not undergo any destruction indicating the importance of the rGO in the Ni-Co LDHs and its role as the backbone for LDHs.

In another attempt to produce a binder-free supercapacitor electrode, Yang et al. (2019) developed a hierarchical Ni-Co LDH/rGO on nickel foam via a solvothermal process. The composite has various merits : (i) upon the addition of rGO in the Ni-Co LDHs the interlayer spacing increases drastically

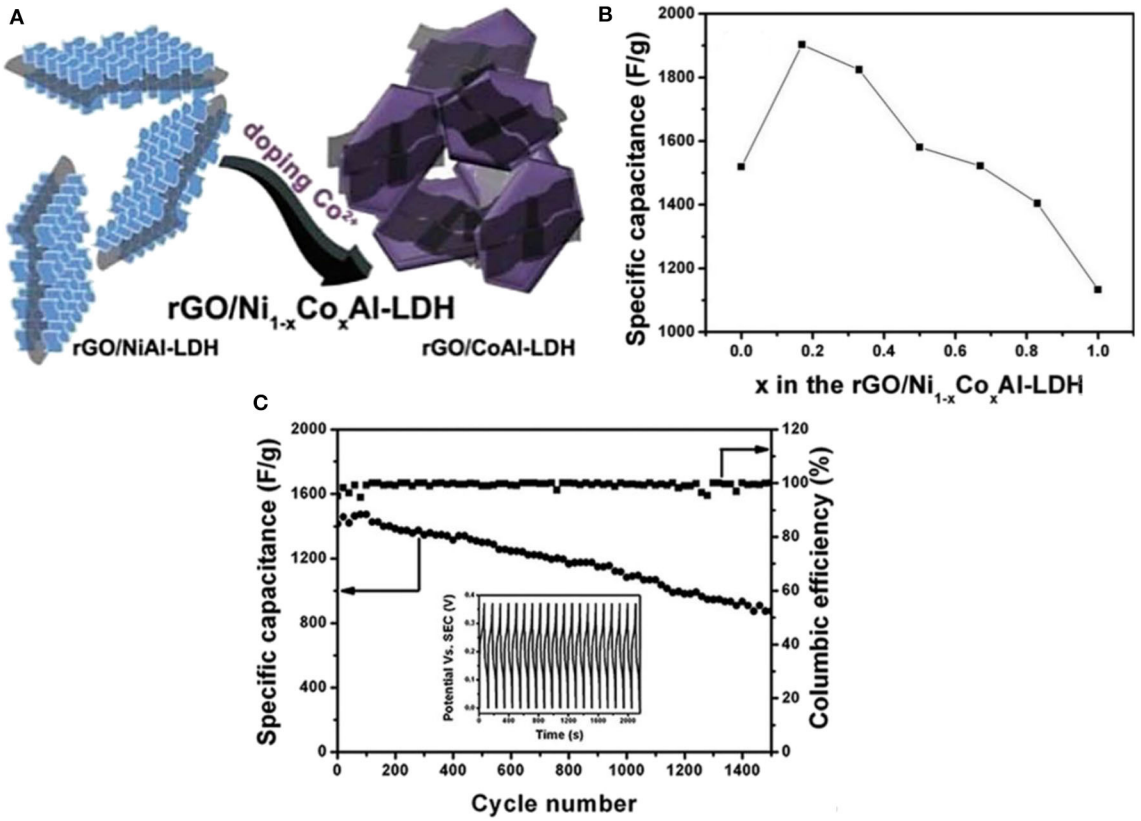

FIGURE 9 | (A) Schematic illustration for the shape conversion from rGO/NiAl-LDHs to the rGO/CoAl-LDHs composite, **(B)** Relationship between the specific capacitance and the doped Co content in rGO/$Ni_{1-x}Co_x$Al-LDHs, and **(C)** The cycling performance and corresponding Coulombic efficiency of rGO/$Ni_{0.83}Co_{0.17}$Al-LDHs at a current density of 10 A g^{-1}. The inset is the first 20 charge-discharge curves (Xu et al., 2014).

promoting the rapid movement of ions and electrons across the sheets; (ii) As the rGO sufficiently decorated within the LDHs, the agglomeration of the composite can be hindered, thereby improves the electrolyte transport to the inner part of the composite; and (iii) the flower-like structure with mesopores on the 2D interconnected nickel foam avoid the formation of "dead volume" which encourage the more active sites to involve in the electrochemical reaction, thus decreases the internal resistance of the composite. The produced asymmetrical supercapacitor device based on Ni-Co LDH/rGO/nickel foam delivered a specific capacitance of 105.62 F g^{-1} at 0.5 A g^{-1} and remarkable specific energy of 40.5 Wh kg^{-1} and a maximum specific power of 4,631 W kg^{-1}.

Another similar composite, Ni-Co LDHs/rGO was prepared via one-pot microwave-assisted synthesis (Kim et al., 2016). It was found that the reaction time, temperature, type of solvent, surfactant and precursor have a profound influence on the size, shape, pore size distribution and crystallinity of Ni-Co LDHs. The different molar ratios of nickel and cobalt also showed a significant effect on the morphology and electrochemical behavior of the composite. Among the different nickel/cobalt ratios, the 2:1 ratio shows the best capacitive performances in a three-electrode system such as the highest specific capacitance (1,622 F g^{-1} at 5 mV s^{-1}) and good cycling stability (80% retention over 5,000 cycles). The improved electrochemical performances of this composite not only originate from the bimetallic hydroxides, but rGO also played an important role in enhancing the overall specific surface area of the composites. In addition, the authors also revealed the influence of nickel and cobalt where nickel controlled the capacitive performance of the composite, while cobalt in maintaining the rate capability of the composite. Likewise, Yan et al. (2014) also reported that the addition of graphene resulted in a high specific surface area of 408.5 m^2 g^{-1} with a pore diameter of 4.75 nm. It also revealed that the basal spacing of the composites increases to 0.86 nm compared to the pristine Ni-Co LDHs, which demonstrated a high specific capacitance 1,980 F g^{-1} at 1 A g^{-1} in a three-electrode system.

Similar findings also were reported by Shahrokhian et al. (2018) in the preparation of electrode material made of Ni-Co LDHs electrodeposited on rGO/nickel foam with excellent supercapacitive performances. In this study, the effect of surfactant cetyltrimethylammonium bromide (CTAB) on the morphology also has been described in detail. The addition of CTAB showed variation in terms of the thickness of Ni-Co LDHs on the rGO/nickel foam. Ni-Co LDHs with CTAB forms thinner

TABLE 4 | Summary of nanocomposites containing carbon-based materials with Ni^{2+}/Co^{2+} LDHs.

Materials		LDH preparation method	Molar ratio of precursor salt (M^{2+}:M^{3+})	C_{sp} (F g^{-1})	SE (Wh kg^{-1})	SP (W kg^{-1})	Electrolyte	Stability	References
+ve electrode	**–ve electrode**								
Carbon nanofibers/Ni-Co-Fe LDHs	Activated carbon	Hydrothermal	Chlorides (5:1:1)	*84.9 (at 1 A g^{-1})	*30.2	*800.1	6 M KOH	*82.7% over 2,000 cycles	Wang et al., 2017a
rGO/NiCoAl LDH	–	Hydrothermal	Nitrates (1:2:1)	#1962 (at 1 A g^{-1})	–	–	6 M KOH	#96.2% over 2,000 cycles	He et al., 2015
rGO/NiCoAl LDH	–	*In-situ* growth	Nitrates (2:1:1)	#1902 (at 1 A g^{-1})	–	–	6 M KOH	#62% over 1,500 cycles	Xu et al., 2014
Graphene sheets/Ni-Co LDHs	–	Microwave heating reflux	Nitrates (2:1)	#1980 (at 1 A g^{-1})	–	–	6 M KOH	#Increase 2.9% over 1,500 cycles	Yan et al., 2014
Ni-Co LDHs/rGO	–	Hydrothermal	Nitrates (1:1)	*151.46 (at 2.5 A g^{-1})	*30.29	*1,500	PVA/KOH gel	*85.6% over 3,000 cycles	Wang et al., 2019a
Ni-Co LDHs/rGO	Activated carbon	Hydrothermal	Nitrates (3:3)	*105.62 (at 0.5 A g^{-1})	*40.54	*206.5	6 M KOH	*94.7% over 8,000 cycles	Yang et al., 2019
N-doped graphene/NiCo LDHs	Activated carbon	Microwave-assisted hydrothermal process	Nitrates (3:2)	*100 (at 0.5 A g^{-1})	*31.2	*354	6 M KOH	*83% over 10,000 cycles	Wang et al., 2019b
Ni-Co LDHs/rGO	–	One-pot microwave-assisted synthesis	Chlorides (2:1)	#1622 (at 5 mV s^{-1})	–	–	6 M KOH	#80% over 5,000 cycles	Kim et al., 2016
Ni-Co LDHs/rGO/nickel foam	rGO/nickel foam	Electrodeposition	Nitrates (1:2)	*233.3 (at 4 A g^{-1})	*68	*4,300	3 M NaOH	#90.5% over 1,000 cycles	Shahrokhian et al., 2018
Ni-Co LDHs/CNTs/nickel foam	–	Chemical bath deposition	Sulfate (1:2)	#1151.2 (at 1 A g^{-1}	–	–	2 M NaOH	#77% over 10,000 cycles	Li et al., 2015b
Ni-Co LDHs/rGO/Ni-Co LDHs/rGO	Activated carbon	Electrodeposition	Nitrates (1:1)	–	*84.9	*424	1 M KOH	*91.6% over 2,000 cycles	Li et al., 2020
Ni-Co LDHs/Ag NP/rGO	Activated carbon	Electrodeposition	Nitrates (1:1)	–	*76	*480	1 M KOH	*79.8% over 5,000 cycles	Li et al., 2019a
Ni-Co LDHs/rGO	Activated carbon	Magnetic stirring	Chlorides (3:2)	#1703 (at 0.5 A g^{-1})	*47.1	*399.9	2 M KOH	*73.3% over 10,000 cycles	Long et al., 2019

#the three-electrode system.
**the two-electrode system.*
C_{sp} is specific capacitance.
SE is a specific energy.
SP is a specific power.

nanosheets compared to hydroxides without CTAB. Moreover, CTAB prevents the formation of bubbles at the solution-electrode interface, thus allowing a uniform formation of Ni-Co LDHs with high porosity on the rGO/nickel foam. In asymmetric assembly, the composite showed good capacitive behavior with a specific energy of 68 Wh kg^{-1} at a specific power of 1,070 W kg^{-1}. The author claimed that the direct deposition of a highly porous thin layer Ni-Co LDHs on highly conductive rGO helps in enhancing the performances.

Li's group (Li et al., 2020) has developed a novel multi-layered Ni-Co LDHs|rGO|Ni-Co LDHs|rGO composite through inkjet printing and electrodeposition method. They employed rGO ink on the nickel foam to form a conductive layer for the electrodeposition of Ni-Co LDHs. Then, the process was continued to form the multi-layered composite. It has been deduced that rGO thin layer on nickel foam not only acts as a conductive scaffold but also provides an excellent charge transfer path in the composite. Moreover, as a conductive scaffold, rGO is also important in forming homogenous nanoflakes of LDHs with good adherence, which are also observed by Guo et al. (2019a). A high energy density of 84.9 Wh kg^{-1} with a maximum power density of 424 W kg^{-1} is achieved by assembling an asymmetrical supercapacitor using this multi-layered Ni-Co LDHs|rGO as the positive electrode and activated carbon as the negative electrode. A similar strategy was also reported by Li et al. (2019a) who have introduced conductive silver nanoparticles (Ag NP) on top of the rGO layer coated on carbon cloth before electrodepositing LDHs. The benefit of Ag NP is to promote conductivity of the composite as Ag NP is known for its high conductivity and excellent chemical stability. This nanocomposite has a high capacity value of 173 mA hg^{-1} at 1 A g^{-1}. The asymmetrical configuration of this nanocomposite delivered a maximum energy density of 76 Wh kg^{-1} at a power density of 480 W kg^{-1}.

With the idea of increasing the capacitive behavior of Ni-Co LDHs/rGO based system, the third transition metal, Al was included (He et al., 2015). The unique nanoflakes structure of Ni-Co-Al LDHs were grown uniformly on the 3D rGO nanosheets created intact contact between the hydroxides and rGO, and subsequently provides better ion movements. The hydroxides may undergo aggregation. However, upon the addition of rGO, such a phenomenon was avoided, resulting in better utilization of both rGO and LDHs in the composites. A study on the content of rGO nanosheets in the composites revealed that the presence of rGO is highly important to increase the specific surface area with desirable pore size distribution generating improved ion transport to the intrinsic space. In a separate study conducted by Xu et al. (2014) showed the influence of the cobalt on the electrochemical performances of Ni-Co LDHs/rGO. At optimized cobalt content of 17%, the composite was able to reach a remarkable specific capacitance of 1,902 F g^{-1} at 1 A g^{-1} in a three-electrode system (**Figure 9**). Both studies disclosed that the synergy between LDHs and rGO promotes electron transport, thus enhance the electrochemical performances. Another work reported by Long et al. (2019) which also used rGO incorporated with Ni-Co LDHs via magnetic stirring. The Ni-Co LDHs/rGO composite with uniform and loose nanostructure exhibited a high specific capacitance of 1,703 F g^{-1} at 0.5 A g^{-1}. The incorporation of rGO greatly helps in preventing aggregation of the Ni-Co hydroxides and, thus improves the supercapacitive performance of the composite. The composite was then tested as a device with activated carbon as the negative electrode. The supercapacitor device demonstrated specific energy as high as 47.1 Wh kg^{-1} and specific power of 399.9 W kg^{-1} (**Figure 10**).

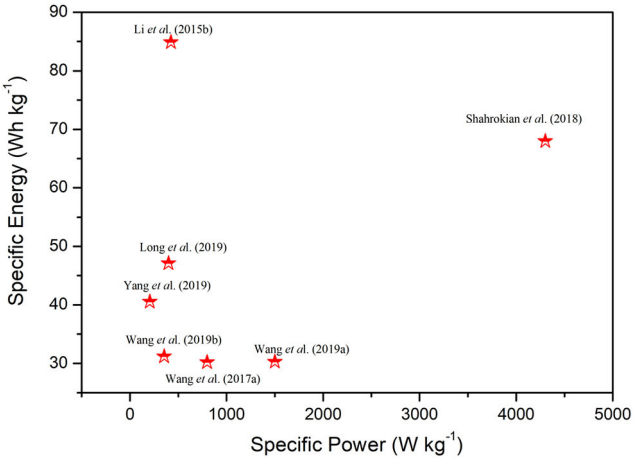

FIGURE 10 | Ragone plot summarizing specific energy and specific power of some of the reported literature on Ni-Co LDHs combining with carbon-based materials.

Instead of using rGO, another work reported on Ni-Co LDHs coated on nitrogen-doped graphene via a simple microwave-assisted hydrothermal process. Two significant improvements were noticed, (a) the good hydrophilicity nature of N-doped graphene serves as good nucleation sites for Ni-Co LDHs growth and (b) N-doped graphene with high conductivity provides large surface area improving the capacitive performance of the composite. The as-prepared composite as a positive electrode and activated carbon as a negative electrode delivers specific energy of 31.2 Wh kg^{-1} at a specific power of 354 W kg^{-1} and extraordinary cycling stability of 83% retention over 10,000 cycles.

In another attempt, Li et al. (2015b) have reported a one-step chemical bath deposition of Ni-Co LDHs nanoflakes uniformly coated on highly porous carbon nanotubes. The functionalized carbon nanotubes acted as a nucleation site for the growth of gauze-like Ni-Co LDHs nanoflakes. The author in this study varied the content of cobalt in the LDHs and found that the rate capabilities increase with the content of cobalt. Three reasons can explain this behavior; (1) the formation of highly conductive CoOOH during oxidation/reduction process, (2) Expansion of interlayer spacing and conductivity due to the presence of intercalated anions and (3) carbon nanotubes as the core in the composite ease the electron transfer in the composite whilst minimizing electrochemical polarization. This hybrid structure shows a maximum specific capacitance of 701 F g^{-1} at a current density of 10 A g^{-1} and a long life span.

SUMMARY AND PERSPECTIVES

In summary, two-dimensional layered double hydroxides, particularly nickel-cobalt layered double hydroxides (Ni-Co LDHs) and their composite with carbon materials have prompted profound research attentions. Benefitting from their unique layered structure, multiple oxidation states of Ni^{2+}/Ni^{3+} and $Co^{2+}/Co^{3+}/Co^{4+}$, exchangeability of interlayer anions and tunability of metal ion ratios, Ni-Co LDHs have gained incredible demand in the field of the supercapacitor. pH and metal ion ratio are the two most prominent factors to be considered to produce LDHs with good crystallinity and phase with desirable morphology. These factors also influence the electrochemical behavior of Ni-Co LDHs and Ni-Co LDHs/carbon-based supercapacitors. The incorporation of carbon-based material into Ni-Co LDHs can help to prevent severe aggregation of Ni-Co LDHs and enhance the supercapacitive performance of the composite due to their high surface area, high conductivity and excellent mechanical strength.

Although there are some encouraging results have been reported on Ni-Co LDHs and Ni-Co LDHs/carbon-based supercapacitors, the development of these electrodes for practical use is still in the early stage. Therefore, substantial measures and action need to be taken to promote the supercapacitor performances of these electrodes, including:

a) Detailed studies on the effects of layered structures, multiple oxidation states, exchangeability of interlayer anions, tunability of metal ion ratio and interlayer spacing of Ni-Co LDHs on the charge storage behavior are much needed. A lot of theoretical understanding of Ni-Co LDHs has been reported, however, advanced and detailed studies on the behavior and charge storage mechanism with respect to the mentioned factors are yet to be found.
b) Knowledge of widening the interlayer spacing of the Ni-Co LDHs are appreciated. Interlayer spacing plays a pivotal role in determining the capacitive behavior of supercapacitors, whereby the larger spacing facilitating the ions intercalation and de-intercalation. Compositing Ni-Co LDHs with carbon-based materials indeed reduces mechanical stress and improves capacitive behavior. However, its impact on interlayer spacing should be explored. It also will be helpful in prolonging the life span of LDHs.

AUTHOR CONTRIBUTIONS

SK wrote the manuscript with the supervision of YS. NA gathered data and organized the manuscript. YS revised the manuscript, edited, and made important supplementary. All authors reviewed the manuscript.

ACKNOWLEDGMENTS

The authors would like to thank Universiti Putra Malaysia for the funding under the research grant of GP-IPS/2017/9580500.

REFERENCES

Abellán, G., Carrasco, J. A., and Coronado, E. (2020). "Layered double hydroxide nanocomposites based on carbon nanoforms," in *Layered Double Hydroxide Polymer Nanocomposites,* eds S. Thomas and S. Daniel (Kidlington: Woodhead Publishing), 411–460.

Albiston, L., Franklin, K. R., Lee, E., and Smeulders, J. B. A. F. (1996). Rheology and microstructure of aqueous layered double hydroxide dispersions. *J. Mater. Chem.* 6, 871–877. doi: 10.1039/jm9960600871

Allmann, R. (1968). The crystal structure of pyroaurite. *Acta Crystallogr. B* 24, 972–977. doi: 10.1107/S0567740868003511

Arias, S., Eon, J. G., San Gil, R. A. S., Licea, Y. E., Palacio, L. A., and Faro, A. C. (2013). Synthesis and characterization of terephthalate-intercalated NiAl layered double hydroxides with high Al content. *Dalton Trans.* 42, 2084–2093. doi: 10.1039/C2DT31502E

Bastakoti, B. P., Huang, H.-S., Chen, L.-C., Wu, K. C. W., and Yamauchi, Y. (2012). Block copolymer assisted synthesis of porous α-Ni(OH)2 microflowers with high surface areas as electrochemical pseudocapacitor materials. *Chem. Commun.* 48, 9150–9152. doi: 10.1039/c2cc32945j

Beaudot, P., De Roy, M. E., and Besse, J. P. (2004). Intercalation of noble metal complexes in LDH compounds. *J. Solid State Chem.* 177, 2691–2698. doi: 10.1016/j.jssc.2004.03.048

Becker, H. I. (1957). *Low Voltage Electrolytic Capacitor*. United States patent application. New York, NY.

Boclair, J. W., Braterman, P. S., Brister, B. D., and Yarberry, F. (1999). Layer–anion interactions in magnesium aluminum layered double hydroxides intercalated with cobalticyanide and nitroprusside. *Chem. Mater.* 11, 2199–2204. doi: 10.1021/cm990148l

BP (2018). *BP Statistical Review of World Energy 2018*. London. Available online at: https://www.bp.com/en/global/corporate/energy-economics/statistical-review-of-world-energy.html

Cai, X., Shen, X., Ma, L., Ji, Z., Xu, C., and Yuan, A. (2015). Solvothermal synthesis of NiCo-layered double hydroxide nanosheets decorated on RGO sheets for high performance supercapacitor. *Chem. Eng. J.* 268, 251–259. doi: 10.1016/j.cej.2015.01.072

Cao, J., Mei, Q., Wu, R., and Wang, W. (2019). Flower-like nickel–cobalt layered hydroxide nanostructures for super long-life asymmetrical supercapacitors. *Electrochim. Acta* 321:134711. doi: 10.1016/j.electacta.2019.134711

Cao, L., Xu, F., Liang, Y.-Y., and Li, H.-L. (2004). Preparation of the novel nanocomposite $Co(OH)_2$/ultra-stable y zeolite and its application as a supercapacitor with high energy density. *Adv. Mater.* 16, 1853–1857. doi: 10.1002/adma.200400183

Cavani, F., Trifirò, F., and Vaccari, A. (1991). Hydrotalcite-type anionic clays: preparation, properties and applications. *Catal. Today* 11, 173–301. doi: 10.1016/0920-5861(91)80068-K

Chang, Z., Wu, C., Song, S., Kuang, Y., Lei, X., Wang, L., et al. (2013). Synthesis mechanism study of layered double hydroxides based on nanoseparation. *Inorg. Chem.* 52, 8694–8698. doi: 10.1021/ic4008763

Chen, G., Liaw, S. S., Li, B., Xu, Y., Dunwell, M., Deng, S., et al. (2014a). Microwave-assisted synthesis of hybrid $Co_xNi_{1-x}(OH)_2$ nanosheets: tuning the composition for high performance supercapacitor. *J. Power Sources* 251, 338–343. doi: 10.1016/j.jpowsour.2013.11.070

Chen, H., Hu, L., Chen, M., Yan, Y., and Wu, L. (2014b). Nickel–cobalt layered double hydroxide nanosheets for high-performance supercapacitor electrode materials. *Adv. Funct. Mater.* 24, 934–942. doi: 10.1002/adfm.201301747

Chen, J., Bradhurst, D. H., Dou, S. X., and Liu, H. K. (1999). Nickel hydroxide as an active material for the positive electrode in rechargeable alkaline batteries. *J. Electrochem. Soc.* 146, 3606–3612. doi: 10.1149/1.1392522

Chen, J.-C., Hsu, C.-T., and Hu, C.-C. (2014c). Superior capacitive performances of binary nickel–cobalt hydroxide nanonetwork prepared by cathodic deposition. *J. Power Sources* 253, 205–213. doi: 10.1016/j.jpowsour.2013.12.073

Cheng, Y., Zhang, H., Varanasi, C. V., and Liu, J. (2013). Improving the performance of cobalt–nickel hydroxide-based self-supporting electrodes

for supercapacitors using accumulative approaches. *Energy Environ. Sci.* 6, 3314–3321. doi: 10.1039/c3ee41143e

Cui, H., Zhao, Y., Ren, W., Wang, M., and Liu, Y. (2013). Large scale selective synthesis of α-$Co(OH)_2$ and β-$Co(OH)_2$ nanosheets through a fluoride ions mediated phase transformation process. *J. Alloys Compd.* 562, 33–37. doi: 10.1016/j.jallcom.2013.02.031

Cullity, B. D. (1957). Elements of X-ray diffraction. *Am. J. Phys.* 25, 394–395. doi: 10.1119/1.1934486

Daud, M., Kamal, M. S., Shehzad, F., and Al-Harthi, M. A. (2016). Graphene/layered double hydroxides nanocomposites: a review of recent progress in synthesis and applications. *Carbon N. Y.* 104, 241–252. doi: 10.1016/j.carbon.2016.03.057

Fan, Z., Yan, J., Wei, T., Zhi, L., Ning, G., Li, T., et al. (2011). Asymmetric supercapacitors based on graphene/MnO_2 and activated carbon nanofiber electrodes with high power and energy density. *Adv. Funct. Mater.* 21, 2366–2375. doi: 10.1002/adfm.201100058

Feitknecht, W., and Gerber, M. (1942). Zur Kenntnis der Doppelhydroxyde und basischen Doppelsalze III. *Über magnesium-aluminiumdoppelhydroxyd. Helvetica Chimica Acta* 25, 131–137. doi: 10.1002/hlca.19420250115

Feng, H.-P., Tang, L., Zeng, G.-M., Tang, J., Deng, Y.-C., Yan, M., et al. (2018). Carbon-based core–shell nanostructured materials for electrochemical energy storage. *J. Mater. Chem. A* 6, 7310–7337. doi: 10.1039/C8TA01257A

Forano, C., Hibino, T., Leroux, F., and Taviot-Guého, C. (2006). "Chapter 13.1 layered double hydroxides," in *Developments in Clay Science,* eds *F. Bergaya, B. K. G. Theng, and* G. Lagaly (Kidlington: Elsevier), 1021–1095.

Gao, Z., Wang, J., Li, Z., Yang, W., Wang, B., Hou, M., et al. (2011). Graphene nanosheet/Ni^{2+}/Al^{3+} layered double-hydroxide composite as a novel electrode for a supercapacitor. *Chem. Mater.* 23, 3509–3516. doi: 10.1021/cm200975x

Ge, X., He, Y., Plachy, T., Kazantseva, N., Saha, P., and Cheng, Q. (2019). Hierarchical PANI/NiCo-LDH core-shell composite networks on carbon cloth for high performance asymmetric supercapacitor. *Nanomaterials* 9:527. doi: 10.3390/nano9040527

Ghadiri, M., Chrzanowski, W., and Rohanizadeh, R. (2015). Biomedical applications of cationic clay minerals. *RSC Adv.* 5, 29467–29481. doi: 10.1039/C4RA16945J

Guo, D., Song, X., Tan, L., Ma, H., Sun, W., Pang, H., et al. (2019a). A facile dissolved and reassembled strategy towards sandwich-like rGO@NiCoAl-LDHs with excellent supercapacitor performance. *Chem. Eng. J.* 356, 955–963. doi: 10.1016/j.cej.2018.09.101

Guo, X., Feng, B., Gai, L., and Zhou, J. (2019b). Reduced graphene oxide/polymer dots-based flexible symmetric supercapacitors delivering an output potential of 1.7 V with electrochemical charge injection. *Electrochim. Acta* 293, 399–407. doi: 10.1016/j.electacta.2018.10.057

Gupta, V., Gupta, S., and Miura, N. (2008). Potentiostatically deposited nanostructured Co_xNi_{1-x} layered double hydroxides as electrode materials for redox-supercapacitors. *J. Power Sources* 175, 680–685. doi: 10.1016/j.jpowsour.2007.09.004

Haas, O., and Cairns, J. E. (1999). Chapter 6. Electrochemical energy storage. *Annu. Rep. C* 95, 163–198. doi: 10.1039/pc095163

Hai-Yan Wang, G.-Q. S. (2018). Layered double hydroxide/graphene composites and their applications for energy storage and conversion. *Acta Phys. Chim. Sin.* 34, 22–35. doi: 10.3866/PKU.WHXB201706302

He, F., Hu, Z., Liu, K., Guo, H., Zhang, S., Liu, H., et al. (2015). Facile fabrication of GNS/NiCoAl-LDH composite as an advanced electrode material for high-performance supercapacitors. *J. Solid State Electrochem.* 19, 607–617. doi: 10.1007/s10008-014-2644-3

Hochstetter, C. (1842). Untersuchung über die zusammensetzung einiger Mineralien. *J. Prakt. Chem.* 27, 375–378. doi: 10.1002/prac.18420270156

Hou, L., Du, Q., Su, L., Di, S., Ma, Z., Chen, L., et al. (2019). Ni-Co layered double hydroxide with self-assembled urchin like morphology for asymmetric supercapacitors. *Mater. Lett.* 237, 262–265. doi: 10.1016/j.matlet.2018.11.123

Hu, Z.-A., Xie, Y.-L., Wang, Y.-X., Wu, H.-Y., Yang, Y.-Y., and Zhang, Z.-Y. (2009). Synthesis and electrochemical characterization of mesoporous CoxNi1–x layered double hydroxides as electrode materials for supercapacitors. *Electrochim. Acta* 54, 2737–2741. doi: 10.1016/j.electacta.2008.11.035

Jeong, Y.-M., Son, I., and Baek, S.-H. (2019). Binder-free of NiCo-layered double hydroxides on Ni-coated textile for wearable and flexible supercapacitors. *Appl. Surf. Sci.* 467–468, 963–967. doi: 10.1016/j.apsusc.2018.10.252

Kameda, T., Saito, M., and Umetsu, Y. (2006). Preparation and characterisation of Mg, Al layered double hydroxides intercalated with 2-naphthalene sulphonate and 2,6-naphthalene disulphonate. *Mater. Trans.* 47, 923–930. doi: 10.2320/matertrans.47.923

Kim, B. K., Sy, S., Yu, A., and Zhang, J. (2015). "Electrochemical supercapacitors for energy storage and conversion," in *Handbook of Clean Energy Systems,* ed J. Yan (Waterloo, ON: John Wiley & Sons, Ltd.), 1–25.

Kim, H.-J., Lee, G. J., Choi, A.-J., Kim, T.-H., Kim, T.-I., and Oh, J.-M. (2018). Layered double hydroxide nanomaterials encapsulating angelica gigas nakai extract for potential anticancer nanomedicine. *Front. Pharmacol.* 9:723. doi: 10.3389/fphar.2018.00723

Kim, I.-H., and Kim, K.-B. (2006). Electrochemical characterization of hydrous ruthenium oxide thin-film electrodes for electrochemical capacitor applications. *J. Electrochem. Soc.* 153, A383–A389. doi: 10.1149/1.2147406

Kim, Y., Cho, E.-S., Park, S.-J., and Kim, S. (2016). One-pot microwave-assisted synthesis of reduced graphene oxide/nickel cobalt double hydroxide composites and their electrochemical behavior. *J. Ind. Eng. Chem.* 33, 108–114. doi: 10.1016/j.jiec.2015.09.023

Kulandaivalu, S., Abdul Shukur, R., and Sulaiman, Y. (2018). Improved electrochemical performance of electrochemically designed layered poly(3,4-ethylenedioxythiophene)/graphene oxide with poly(3,4-ethylenedioxythiophene)/nanocrystalline cellulose nanocomposite. *Synth. Met.* 245, 24–31. doi: 10.1016/j.synthmet.2018.08.002

Kulandaivalu, S., Hussein, M. Z., Jaafar, A. M., Mohd, M. A. A., Azman, N. H. N., and Sulaiman, Y. (2019). A simple strategy to prepare a layer-by-layer assembled composite of Ni–Co LDHs on polypyrrole/rGO for a high specific capacitance supercapacitor. *RSC Adv.* 9, 40478–40486. doi: 10.1039/C9RA08134H

Kulandaivalu, S., and Sulaiman, Y. (2019). Recent advances in layer-by-layer assembled conducting polymer based composites for supercapacitors. *Energies* 12:2107. doi: 10.3390/en12112107

Kulkarni, S. B., Jagadale, A. D., Kumbhar, V. S., Bulakhe, R. N., Joshi, S. S., and Lokhande, C. D. (2013). Potentiodynamic deposition of composition influenced $Co_{1-x}Ni_x$ LDHs thin film electrode for redox supercapacitors. *Int. J. Hydr. Energy* 38, 4046–4053. doi: 10.1016/j.ijhydene.2013.01.047

Lai, X., Halpert, J. E., and Wang, D. (2012). Recent advances in micro-/nano-structured hollow spheres for energy applications: from simple to complex systems. *Energy Environ. Sci.* 5, 5604–5618. doi: 10.1039/C1EE02426D

Largeot, C., Portet, C., Chmiola, J., Taberna, P. L., Gogotsi, Y., and Simon, P. (2008). Relation between the ion size and pore size for an electric double-layer capacitor. *J. Am. Chem. Soc.* 130, 2730–2731. doi: 10.1021/ja7106178

Li, C., Wang, G., Evans, D. G., and Duan, X. (2004). Incorporation of rare-earth ions in Mg–Al layered double hydroxides: intercalation with an [Eu(EDTA)]–chelate. *J. Solid State Chem.* 177, 4569–4575. doi: 10.1016/j.jssc.2004.09.005

Li, K., Kumada, N., Yonesaki, Y., Takei, T., Kinomura, N., Wang, H., et al. (2010). The pH effects on the formation of Ni/Al nitrate form layered double hydroxides (LDHs) by chemical precipitation and hydrothermal method. *Mater. Chem. Phys.* 121, 223–229. doi: 10.1016/j.matchemphys.2010.01.026

Li, L., Hui, K. S., Hui, K. N., and Cho, Y.-R. (2017a). Ultrathin petal-like NiAl layered double oxide/sulfide composites as an advanced electrode for high-performance asymmetric supercapacitors. *J. Mater. Chem. A* 5, 19687–19696. doi: 10.1039/C7TA06119F

Li, M., Cheng, J. P., Fang, J. H., Yang, Y., Liu, F., and Zhang, X. B. (2014). NiAl-layered double hydroxide/reduced graphene oxide composite: microwave-assisted synthesis and supercapacitive properties. *Electrochim. Acta* 134, 309–318. doi: 10.1016/j.electacta.2014.04.141

Li, M., Cheng, J. P., Wang, J., Liu, F., and Zhang, X. B. (2016a). The growth of nickel-manganese and cobalt-manganese layered double hydroxides on reduced graphene oxide for supercapacitor. *Electrochim. Acta* 206, 108–115. doi: 10.1016/j.electacta.2016.04.084

Li, M., Liu, F., Cheng, J. P., Ying, J., and Zhang, X. B. (2015a). Enhanced performance of nickel–aluminum layered double hydroxide nanosheets/carbon nanotubes composite for supercapacitor and asymmetric capacitor. *J. Alloys Compd.* 635, 225–232. doi: 10.1016/j.jallcom.2015.02.130

Li, M., Liu, F., Zhang, X. B., and Cheng, J. P. (2016b). A comparative study of Ni–Mn layered double hydroxide/carbon composites with different morphologies for supercapacitors. *Phys. Chem. Chem. Phys.* 18, 30068–30078. doi: 10.1039/C6CP05119G

Li, M., Ma, K. Y., Cheng, J. P., Lv, D., and Zhang, X. B. (2015b). Nickel–cobalt hydroxide nanoflakes conformal coating on carbon nanotubes as a supercapacitive material with high-rate capability. *J. Power Sources* 286, 438–444. doi: 10.1016/j.jpowsour.2015.04.013

Li, Q., Lu, C., Chen, C., Xie, L., Liu, Y., Li, Y., et al. (2017b). Layered $NiCo_2O_4$/reduced graphene oxide composite as an advanced electrode for supercapacitor. *Energy Storage Mater.* 8, 59–67. doi: 10.1016/j.ensm.2017.04.002

Li, S., Wang, F., Jing, X., Wang, J., Saba, J., Liu, Q., et al. (2012a). Synthesis of layered double hydroxides from eggshells. *Mater. Chem. Phys.* 132, 39–43. doi: 10.1016/j.matchemphys.2011.10.049

Li, T., Li, G. H., Li, L. H., Liu, L., Xu, Y., Ding, H. Y., et al. (2016c). Large-scale self-assembly of 3D flower-like hierarchical Ni/Co-LDHs microspheres for high-performance flexible asymmetric supercapacitors. *ACS Appl. Mater. Interfaces* 8, 2562–2572. doi: 10.1021/acsami.5b10158

Li, W., Livi, K. J. T., Xu, W., Siebecker, M. G., Wang, Y., Phillips, B. L., et al. (2012b). Formation of crystalline Zn–Al layered double hydroxide precipitates on γ-Alumina: the role of mineral dissolution. *Environ. Sci. Technol.* 46, 11670–11677. doi: 10.1021/es3018094

Li, X., Du, D., Zhang, Y., Xing, W., Xue, Q., and Yan, Z. (2017c). Layered double hydroxides toward high-performance supercapacitors. *J. Mater. Chem. A* 5, 15460–15485. doi: 10.1039/C7TA04001F

Li, X., Zhao, Y., Yu, J., Liu, Q., Chen, R., Zhang, H., et al. (2019a). Layer-by-layer inkjet printing GO film and Ag nanoparticles supported nickel cobalt layered double hydroxide as a flexible and binder-free electrode for supercapacitors. *J. Colloid Interface Sci.* 557, 691–699. doi: 10.1016/j.jcis.2019.09.063

Li, X., Zhao, Y., Yu, J., Liu, Q., Chen, R., Zhang, H., et al. (2020). Layer by layer inkjet printing reduced graphene oxide film supported nickel cobalt layered double hydroxide as a binder-free electrode for supercapacitors. *Appl. Surf. Sci.* 509:144872. doi: 10.1016/j.apsusc.2019.144872

Li, Y., Yuan, X., Yang, H., Chao, Y., Guo, S., and Wang, C. (2019b). One-step synthesis of silver nanowires with ultra-long length and thin diameter to make flexible transparent conductive films. *Materials*12:401. doi: 10.3390/ma12030401

Liu, J., Wang, J., Xu, C., Jiang, H., Li, C., Zhang, L., et al. (2018a). Advanced energy storage devices: basic principles, analytical methods, and rational materials design. *Adv. Sci.* 5:1700322. doi: 10.1002/advs.201700322

Liu, L., Niu, Z., and Chen, J. (2016). Unconventional supercapacitors from nanocarbon-based electrode materials to device configurations. *Chem. Soc. Rev.* 45, 4340–4363. doi: 10.1039/C6CS00041J

Liu, T., Zhang, L., You, W., and Yu, J. (2018b). Core–shell nitrogen-doped carbon hollow spheres/co_3o_4 nanosheets as advanced electrode for high-performance supercapacitor. *Small* 14:1702407. doi: 10.1002/smll.201702407

Liu, X., Ma, R., Bando, Y., and Sasaki, T. (2012). A general strategy to layered transition-metal hydroxide nanocones: tuning the composition for high electrochemical performance. *Adv. Mater.* 24, 2148–2153. doi: 10.1002/adma.201104753

Liu, Y., Fu, N., Zhang, G., Xu, M., Lu, W., Zhou, L., et al. (2017). Design of hierarchical Ni-Co@Ni-Co layered double hydroxide core–shell structured nanotube array for high-performance flexible all-solid-state battery-type supercapacitors. *Adv. Funct. Mater.* 27:1605307. doi: 10.1002/adfm.201605307

Lobato, B., Suárez, L., Guardia, L., and Centeno, T. A. (2017). Capacitance and surface of carbons in supercapacitors. *Carbon N. Y.* 122, 434–445. doi: 10.1016/j.carbon.2017.06.083

Long, D., Liu, H., Yuan, Y., Li, J., Li, Z., and Zhu, J. (2019). A facile and large-scale synthesis of NiCo-LDHs@rGO composite for high performance asymmetric supercapacitors. *J. Alloys Compd.* 805, 1096–1105. doi: 10.1016/j.jallcom.2019.07.161

Long, X., Li, J., Xiao, S., Yan, K., Wang, Z., Chen, H., et al. (2014). A strongly coupled graphene and feni double hydroxide hybrid as an excellent electrocatalyst for the oxygen evolution reaction. *Angew. Chem Int Ed.* 53, 7584–7588. doi: 10.1002/anie.201402822

Luan, F., Wang, G., Ling, Y., Lu, X., Wang, H., Tong, Y., et al. (2013). High energy density asymmetric supercapacitors with a nickel oxide nanoflake cathode and a 3D reduced graphene oxide anode. *Nanoscale* 5, 7984–7990. doi: 10.1039/c3nr02710d

Mahjoubi, F. Z., Khalidi, A., Abdennouri, M., and Barka, N. (2017). Zn–Al layered double hydroxides intercalated with carbonate, nitrate, chloride and sulphate ions: synthesis, characterisation and dye removal properties. *J. Taibah Univ. Sci.* 11, 90–100. doi: 10.1016/j.jtusci.2015.10.007

Mehrabimatin, B., Gilshteyn, E. P., Melandsø Buan, M. E., Sorsa, O., Jiang, H., Iraji Zad, A., et al. (2019). Flexible and mechanically durable asymmetric supercapacitor based on NiCo layered double hydroxide and nitrogen-doped graphene using a simple fabrication method. *Energy Technol.* 7:1801002. doi: 10.1002/ente.201801002

Meng, X., and Deng, D. (2016). Bio-inspired synthesis of α-$Ni(OH)_2$ nanobristles on various substrates and their applications. *J. Mater. Chem. A* 4, 6919–6925. doi: 10.1039/C5TA09329E

Miyata, S. (1975). The syntheses of hydrotalcite-likecompounds and their structures and physico-chemical properties i: the systems Mg^{2+}-Al^{3+}-NO_3^-, Mg^{2+}-Al^{3+}-Cl^-, Mg^{2+}-Al^{3+}-ClO_4^-, Ni^{2+}-Al^{3+}-Cl^- and Zn^{2+}-Al^{3+}-Cl^-. *Clays Clay Miner.* 23, 369–375. doi: 10.1346/CCMN.1975.0230508

Mohd Abdah, M. A., Mohammed Modawe Aldris Edris, N., Kulandaivalu, S., Abdul Rahman, N., and Sulaiman, Y. (2018a). Supercapacitor with superior electrochemical properties derived from symmetrical manganese oxide-carbon fiber coated with polypyrrole. *Int. J. Hydrogen Energy* 43, 17328–17337. doi: 10.1016/j.ijhydene.2018.07.093

Mohd Abdah, M. A., Mohd Razali, N. S., Lim, P. T., Kulandaivalu, S., and Sulaiman, Y. (2018b). One-step potentiostatic electrodeposition of polypyrrole/graphene oxide/multi-walled carbon nanotubes ternary nanocomposite for supercapacitor. *Mater. Chem. Phys.* 219, 120–128. doi: 10.1016/j.matchemphys.2018.08.018

Motori, A., Sandrolini, F., and Davolio, G. (1994). Electrical properties of nickel hydroxide for alkaline cell systems. *J. Power Sources* 48, 361–370. doi: 10.1016/0378-7753(94)80032-4

Nagaraju, G., Chandra Sekhar, S., Krishna Bharat, L., and Yu, J. S. (2017). Wearable fabrics with self-branched bimetallic layered double hydroxide coaxial nanostructures for hybrid supercapacitors. *ACS Nano* 11, 10860–10874. doi: 10.1021/acsnano.7b04368

Nagaraju, G., Raju, G. S. R., Ko, Y. H., and Yu, J. S. (2016). Hierarchical Ni–Co layered double hydroxide nanosheets entrapped on conductive textile fibers: a cost-effective and flexible electrode for high-performance pseudocapacitors. *Nanoscale* 8, 812–825. doi: 10.1039/C5NR05643H

Nguyen, T., Boudard, M., João Carmezim, M., and Fátima Montemor, M. (2017). $Ni_xCo_{1-x}(OH)_2$ nanosheets on carbon nanofoam paper as high areal capacity electrodes for hybrid supercapacitors. *Energy* 126, 208–216. doi: 10.1016/j.energy.2017.03.024

Oh, J.-M., Hwang, S.-H., and Choy, J.-H. (2002). The effect of synthetic conditions on tailoring the size of hydrotalcite particles. *Solid State Ionics* 151, 285–291. doi: 10.1016/S0167-2738(02)00725-7

Pan, Z., Sun, H., Pan, J., Zhang, J., Wang, B., and Peng, H. (2018). The creation of hollow walls in carbon nanotubes for high-performance lithium ion batteries. *Carbon N. Y.* 133, 384–389. doi: 10.1016/j.carbon.2018.03.021

Pandolfo, A. G., and Hollenkamp, A. F. (2006). Carbon properties and their role in supercapacitors. *J. Power Sources* 157, 11–27. doi: 10.1016/j.jpowsour.2006.02.065

Pausch, I., Lohse, H.-H., Schürmann, K., and Allmann, R. (1986). Syntheses of disordered and Al-Rich hydrotalcite-like compounds. *Clays Clay Miner.* 34, 507–510. doi: 10.1346/CCMN.1986.0340502

Pu, J., Tong, Y., Wang, S., Sheng, E., and Wang, Z. (2014). Nickel–cobalt hydroxide nanosheets arrays on Ni foam for pseudocapacitor applications. *J. Power Sources* 250, 250–256. doi: 10.1016/j.jpowsour.2013.10.108

Qin, Q., Ou, D., Ye, C., Chen, L., Lan, B., Yan, J., et al. (2019). Systematic study on hybrid supercapacitor of Ni-Co layered double hydroxide//activated carbons. *Electrochim. Acta* 305, 403–415. doi: 10.1016/j.electacta.2019.03.082

Qiu, Z., Peng, Y., He, D., Wang, Y., and Chen, S. (2018). Ternary Fe_3O_4@C@PANi nanocomposites as high-performance supercapacitor electrode materials. *J. Mater. Sci.* 53, 12322–12333. doi: 10.1007/s10853-018-2451-9

Richetta, M., Varone, A., Mattoccia, A., Medaglia, P. G., Kaciulis, S., Mezzi, A., et al. (2018). Preparation, intercalation, and characterization of nanostructured (Zn, Al) layered double hydroxides (LDHs). *Surf. Interf. Anal.* 50, 1094–1098. doi: 10.1002/sia.6468

Sarfraz, M., and Shakir, I. (2017). Recent advances in layered double hydroxides as electrode materials for high-performance electrochemical energy storage devices. *J. Energy Stor.* 13, 103–122. doi: 10.1016/j.est.2017.06.011

Shahrokhian, S., Rahimi, S., and Mohammadi, R. (2018). Nickel-cobalt layered double hydroxide ultrathin nanosheets coated on reduced graphene oxide nonosheets/nickel foam for high performance asymmetric supercapacitors. *Int. J. Hydrogen Energy* 43, 2256–2267. doi: 10.1016/j.ijhydene.2017.12.019

Shao, M., Wei, M., Evans, D. G., and Duan, X. (2015). "Layered double hydroxide materials in photocatalysis," in *Photofunctional Layered Materials,* eds *D. Yan and M. Wei (Cham: Springer International Publishing)*, 105–136.

Shen, J., Ye, S., Xu, X., Liang, J., He, G., and Chen, H. (2019). Reduced graphene oxide based NiCo layered double hydroxide nanocomposites: an efficient catalyst for epoxidation of styrene. *Inorg. Chem. Commun.* 104, 219–222. doi: 10.1016/j.inoche.2019.03.044

Shi, W., Zhu, J., Sim, D. H., Tay, Y. Y., Lu, Z., Zhang, X., et al. (2011). Achieving high specific charge capacitances in Fe_3O_4/reduced graphene oxide nanocomposites. *J. Mater. Chem.* 21, 3422–3427. doi: 10.1039/c0jm03175e

Simon, P., and Gogotsi, Y. (2008). Materials for electrochemical capacitors. *Nat. Mater.* 7, 845–854. doi: 10.1038/nmat2297

Singh, Z. (2016). Applications and toxicity of graphene family nanomaterials and their composites. *Nanotechnol. Sci. Appl.* 9, 15–28. doi: 10.2147/NSA.S101818

Sun, P., Yi, H., Peng, T., Jing, Y., Wang, R., Wang, H., et al. (2017). Ultrathin MnO_2 nanoflakes deposited on carbon nanotube networks for symmetrical supercapacitors with enhanced performance. *J. Power Sources* 341, 27–35. doi: 10.1016/j.jpowsour.2016.11.112

Sun, X., Neuperger, E., and Dey, S. K. (2015). Insights into the synthesis of layered double hydroxide (LDH) nanoparticles: part 1. *Optimization and controlled synthesis of chloride-intercalated LDH. J Colloid Interface Sci.* 459, 264–272. doi: 10.1016/j.jcis.2015.07.073

Sun, X., Wang, G., Sun, H., Lu, F., Yu, M., and Lian, J. (2013). Morphology controlled high performance supercapacitor behaviour of the Ni–Co binary hydroxide system. *J. Power Sources* 238, 150–156. doi: 10.1016/j.jpowsour.2013.03.069

Taylor, H. F. W. (2018). Segregation and cation-ordering in sjögrenite and pyroaurite. *Mineral. Mag.* 37, 338–342. doi: 10.1180/minmag.1969.037.287.04

Tiwari, J. N., Tiwari, R. N., and Kim, K. S. (2012). Zero-dimensional, one-dimensional, two-dimensional and three-dimensional nanostructured materials for advanced electrochemical energy devices. *Prog. Mater. Sci.* 57, 724–803. doi: 10.1016/j.pmatsci.2011.08.003

Vaccari, A. (1998). Preparation and catalytic properties of cationic and anionic clays. *Catal. Today* 41, 53–71. doi: 10.1016/S0920-5861(98)00038-8

Varadwaj, G. B. B., and Nyamori, V. O. (2016). Layered double hydroxide- and graphene-based hierarchical nanocomposites: synthetic strategies and promising applications in energy conversion and conservation. *Nano Res.* 9, 3598–3621. doi: 10.1007/s12274-016-1250-3

Vellacheri, R., Pillai, V. K., and Kurungot, S. (2012). Hydrous RuO_2-carbon nanofiber electrodes with high mass and electrode-specific capacitance for efficient energy storage. *Nanoscale* 4, 890–896. doi: 10.1039/C2NR11479H

Walton, R. I. (2018). "Double hydroxides: present and future," in *Clay Minerals. Cambridge University Press*, ed V. Rives (New York, NY), 139–139.

Wang, C., Zhang, X., Sun, X., and Ma, Y. (2016). Facile fabrication of ethylene glycol intercalated cobalt-nickel layered double hydroxide nanosheets supported on nickel foam as flexible binder-free electrodes for advanced electrochemical energy storage. *Electrochim. Acta* 191, 329–336. doi: 10.1016/j.electacta.2015.12.154

Wang, D., Wei, A., Tian, L., Mensah, A., Li, D., Xu, Y., et al. (2019a). Nickel-cobalt layered double hydroxide nanosheets with reduced graphene oxide grown on carbon cloth for symmetric supercapacitor. *Appl. Surf. Sci.* 483, 593–600. doi: 10.1016/j.apsusc.2019.03.345

Wang, F., Sun, S., Xu, Y., Wang, T., Yu, R., and Li, H. (2017a). High performance asymmetric supercapacitor based on cobalt nickle iron-layered double hydroxide/carbon nanofibres and activated carbon. *Sci. Rep.* 7:4707. doi: 10.1038/s41598-017-04807-1

Wang, F., Wang, T., Sun, S., Xu, Y., Yu, R., and Li, H. (2018a). One-step synthesis of nickle iron-layered double hydroxide/reduced graphene oxide/carbon nanofibres composite as electrode materials for asymmetric supercapacitor. *Sci. Rep.* 8:8908. doi: 10.1038/s41598-018-27171-0

Wang, G., Zhang, L., and Zhang, J. (2012). A review of electrode materials for electrochemical supercapacitors. *Chem. Soc. Rev.* 41, 797–828. doi: 10.1039/C1CS15060J

Wang, J., Wang, L., Chen, X., Lu, Y., and Yang, W. (2015). Chemical power source based on layered double hydroxides. *J. Solid State Electrochem.* 19, 1933–1948. doi: 10.1007/s10008-014-2723-5

Wang, Q., Gao, Y., Luo, J., Zhong, Z., Borgna, A., Guo, Z., et al. (2013a). Synthesis of nano-sized spherical Mg3Al–CO3 layered double hydroxide as a high-temperature CO_2 adsorbent. *RSC Adv.* 3, 3414–3420. doi: 10.1039/c2ra22607c

Wang, T., Liu, X., Ma, C., Liu, Y., Dong, H., Ma, W., et al. (2018b). 3D Ag/NiCo-layered double hydroxide with adsorptive and photocatalytic performance. *J. Taiwan Inst. Chem. Eng.* 93, 298–305. doi: 10.1016/j.jtice.2018.07.031

Wang, T., Zhang, S., Yan, X., Lyu, M., Wang, L., Bell, J., et al. (2017b). 2-Methylimidazole-Derived Ni–Co layered double hydroxide nanosheets as high rate capability and high energy density storage material in hybrid supercapacitors. *ACS Appl. Mater. Interfaces* 9, 15510–15524. doi: 10.1021/acsami.7b02987

Wang, W., Zhang, N., Ye, Z., Hong, Z., and Zhi, M. (2019b). Synthesis of 3D hierarchical porous Ni–Co layered double hydroxide/N-doped reduced graphene oxide composites for supercapacitor electrodes. *Inorg. Chem. Front.* 6, 407–416. doi: 10.1039/C8QI01132J

Wang, X., and Liu, T. (2011). Fabrication and characterization of ultrathin graphene oxide/Poly(vinyl alcohol) composite films via layer-by-layer assembly. *J. Macromol. Sci. B* 50, 1098–1107. doi: 10.1080/00222348.2010.497694

Wang, Y., Shang, B., Lin, F., Chen, Y., Ma, R., Peng, B., et al. (2018c). Controllable synthesis of hierarchical nickel hydroxide nanotubes for high performance supercapacitors. *Chem. Commun.* 54, 559–562. doi: 10.1039/C7CC08879E

Wang, Y., Wu, P., Li, Y., Zhu, N., and Dang, Z. (2013b). Structural and spectroscopic study of tripeptide/layered double hydroxide hybrids. *J. Colloid Interface Sci.* 394, 564–572. doi: 10.1016/j.jcis.2012.11.031

Wang, Y.-F., Wang, H.-T., Yang, S.-Y., Yue, Y., and Bian, S.-W. (2019c). Hierarchical NiCo2S4@Nickel–cobalt layered double hydroxide nanotube arrays on metallic cotton yarns for flexible supercapacitors. *ACS Appl. Mater. Interfaces* 11, 30384–30390. doi: 10.1021/acsami.9b06317

Wei, M., Huang, Q., Zhou, Y., Peng, Z., and Chu, W. (2018). Ultrathin nanosheets of cobalt-nickel hydroxides hetero-structure via electrodeposition and precursor adjustment with excellent performance for supercapacitor. *J. Energy Chem.* 27, 591–599. doi: 10.1016/j.jechem.2017.10.022

Wen, J., Li, S., Chen, T., Yue, Y., Liu, N., Gao, Y., et al. (2016). Three-dimensional hierarchical NiCo hydroxide@Ni3S2 nanorod hybrid structure as high performance positive material for asymmetric supercapacitor. *Electrochim. Acta* 222, 965–975. doi: 10.1016/j.electacta.2016.11.064

Weng, B., Liu, S., Tang, Z.-R., and Xu, Y.-J. (2014). One-dimensional nanostructure based materials for versatile photocatalytic applications. *RSC Adv.* 4, 12685–12700. doi: 10.1039/c3ra47910b

Windisch, C. F., Exarhos, G. J., Ferris, K. F., Engelhard, M. H., and Stewart, D. C. (2001). Infrared transparent spinel films with p-type conductivity. *Thin Solid Films* 398–399, 45–52. doi: 10.1016/S0040-6090(01)01302-5

Wu, S., Guo, H., Hui, K. S., and Hui, K. N. (2019a). Rational design of integrated CuO@$Co_xNi_{1-x}(OH)_2$ nanowire arrays on copper foam for high-rate and long-life supercapacitors. *Electrochim. Acta* 295, 759–768. doi: 10.1016/j.electacta.2018.10.183

Wu, X., Lian, M., and Wang, Q. (2019b). A high-performance asymmetric supercapacitors based on hydrogen bonding nanoflower-like polypyrrole and NiCo(OH)2 electrode materials. *Electrochim. Acta* 295, 655–661. doi: 10.1016/j.electacta.2018.10.199

Xia, D., Chen, H., Jiang, J., Zhang, L., Zhao, Y., Guo, D., et al. (2015). Facilely synthesized α phase nickel–cobalt bimetallic hydroxides: Tuning the composition for high pseudocapacitance. *Electrochim. Acta* 156, 108–114. doi: 10.1016/j.electacta.2015.01.018

Xie, L., Hu, Z., Lv, C., Sun, G., Wang, J., Li, Y., et al. (2012). CoxNi1–x double hydroxide nanoparticles with ultrahigh specific capacitances as supercapacitor electrode materials. *Electrochim. Acta* 78, 205–211. doi: 10.1016/j.electacta.2012.05.145

Xu, J., Gai, S., He, F., Niu, N., Gao, P., Chen, Y., et al. (2014). Reduced graphene oxide/Ni1-xCoxAl-layered double hydroxide composites: preparation

and high supercapacitor performance. *Dalton Trans.* 43, 11667–11675. doi: 10.1039/C4DT00686K

Xu, J., Liao, K., Song, K., Wu, J., Hu, X., Gao, H., et al. (2018). Fast *in situ* synthesis of CoFe layered double hydroxide onto multi-layer graphene for electrochemical capacitors. *J. Solid State Electrochem.* 22, 1037–1045. doi: 10.1007/s10008-017-3839-1

Xu, Z. P., Stevenson, G., Lu, C.-Q., and Lu, G. Q. (2006). Dispersion and size control of layered double hydroxide nanoparticles in aqueous solutions. *J. Phys. Chem. B* 110, 16923–16929. doi: 10.1021/jp062281o

Yan, A.-L., Wang, X.-C., and Cheng, J.-P. (2018). Research progress of NiMn layered double hydroxides for supercapacitors: a review. *Nanomaterials* 8:747. doi: 10.3390/nano8100747

Yan, T., Li, R., and Li, Z. (2014). Nickel–cobalt layered double hydroxide ultrathin nanoflakes decorated on graphene sheets with a 3D nanonetwork structure as supercapacitive materials. *Mater. Res. Bull.* 51, 97–104. doi: 10.1016/j.materresbull.2013.11.044

Yan, T., Li, R., Yang, T., and Li, Z. (2015). Nickel/cobalt layered double hydroxide hollow microspheres with hydrangea-like morphology for high-performance supercapacitors. *Electrochim. Acta* 152, 530–537. doi: 10.1016/j.electacta.2014.08.149

Yang, S., Zhang, Z., Zhou, J., Sui, Z., and Zhou, X. (2019). Hierarchical NiCo LDH–rGO/Ni foam composite as electrode material for high-performance supercapacitors. *Trans. Tianjin Univ.* 25, 266–275. doi: 10.1007/s12209-018-0180-4

Yang, W., Gao, Z., Wang, J., Ma, J., Zhang, M., and Liu, L. (2013). Solvothermal one-step synthesis of Ni–Al layered double hydroxide/carbon nanotube/reduced graphene oxide sheet ternary nanocomposite with ultrahigh capacitance for supercapacitors. *ACS Appl. Mater. Interfaces* 5, 5443–5454. doi: 10.1021/am4003843

Yang, Y. J., and Li, W. (2019). Hierarchical Ni–Co double hydroxide nanosheets on reduced graphene oxide self-assembled on Ni foam for high-energy hybrid supercapacitors. *J. Alloys Compd.* 776, 543–553. doi: 10.1016/j.jallcom.2018.10.344

Young, C., Lin, J., Wang, J., Ding, B., Zhang, X., Alshehri, S. M., et al. (2018). Significant effect of pore sizes on energy storage in nanoporous carbon supercapacitors. *Chem. A Eur. J.* 24, 6127–6132. doi: 10.1002/chem.201705465

Yu, Z., Tetard, L., Zhai, L., and Thomas, J. (2015). Supercapacitor electrode materials: nanostructures from 0 to 3 dimensions. *Energy Environ. Sci.* 8, 702–730. doi: 10.1039/C4EE03229B

Yulian, N., Ruiyi, L., Zaijun, L., Yinjun, F., and Junkang, L. (2013). High-performance supercapacitors materials prepared via *in situ* growth of NiAl-layered double hydroxide nanoflakes on well-activated graphene nanosheets. *Electrochim. Acta* 94, 360–366. doi: 10.1016/j.electacta.2012.09.084

Zhang, J., Zheng, Z., Wu, G., and Hua, Q. (2019). Hierarchical electrodes assembled by alternate NiCo hydroxide nanowires arrays and conductive interlayers with enhanced properties for electrochemical supercapacitors. *J. Alloys Compd.* 785, 725–731. doi: 10.1016/j.jallcom.2019.01.233

Zhang, L., Zhang, X., Shen, L., Gao, B., Hao, L., Lu, X., et al. (2012). Enhanced high-current capacitive behavior of graphene/CoAl-layered double hydroxide composites as electrode material for supercapacitors. *J. Power Sources* 199, 395–401. doi: 10.1016/j.jpowsour.2011.10.056

Zhang, W., Ma, C., Fang, J., Cheng, J., Zhang, X., Dong, S., et al. (2013). Asymmetric electrochemical capacitors with high energy and power density based on graphene/CoAl-LDH and activated carbon electrodes. *RSC Adv.* 3, 2483–2490. doi: 10.1039/c2ra2 3283a

Zhao, J., Xu, S., Tschulik, K., Compton, R. G., Wei, M., O'hare, D., et al. (2015). Molecular-scale hybridization of clay monolayers and conducting polymer for thin-film supercapacitors. *Adv. Funct. Mater.* 25, 2745–2753. doi: 10.1002/adfm.201500408

Zhao, M., Zhao, Q., Li, B., Xue, H., Pang, H., and Chen, C. (2017). Recent progress in layered double hydroxide based materials for electrochemical capacitors: design, synthesis and performance. *Nanoscale* 9, 15206–15225. doi: 10.1039/C7NR04752E

Zhao, Y., Xiao, F., and Jiao, Q. (2011). Hydrothermal synthesis of Ni/Al layered double hydroxide nanorods. *J. Nanotechnol* 2011: 6. doi: 10.1155/2011/646409

Zhi, M., Xiang, C., Li, J., Li, M., and Wu, N. (2013). Nanostructured carbon–metal oxide composite electrodes for supercapacitors: a review. *Nanoscale* 5, 72–88. doi: 10.1039/C2NR32040A

Zhong, C., Deng, Y., Hu, W., Qiao, J., Zhang, L., and Zhang, J. (2015). A review of electrolyte materials and compositions for electrochemical supercapacitors. *Chem. Soc. Rev.* 44, 7484–7539. doi: 10.1039/C5CS0 0303B

Conflict of Interest: The authors declare that the research was conducted in the absence of any commercial or financial relationships that could be construed as a potential conflict of interest.